Energy dependence and fluctuations of anisotropic flow in Pb–Pb collisions at $\sqrt{s_{\mathrm{NN}}} = 5.02$ and 2.76 TeV

The ALICE collaboration

E-mail: ALICE-publications@cern.ch

ABSTRACT: Measurements of anisotropic flow coefficients with two- and multi-particle cumulants for inclusive charged particles in Pb–Pb collisions at $\sqrt{s_{\mathrm{NN}}} = 5.02$ and 2.76 TeV are reported in the pseudorapidity range $|\eta| < 0.8$ and transverse momentum $0.2 < p_{\mathrm{T}} < 50\,\mathrm{GeV}/c$. The full data sample collected by the ALICE detector in 2015 (2010), corresponding to an integrated luminosity of 12.7 (2.0) $\mu\mathrm{b}^{-1}$ in the centrality range 0–80%, is analysed. Flow coefficients up to the sixth flow harmonic (v_6) are reported and a detailed comparison among results at the two energies is carried out. The p_{T} dependence of anisotropic flow coefficients and its evolution with respect to centrality and harmonic number n are investigated. An approximate power-law scaling of the form $v_n(p_{\mathrm{T}}) \sim p_{\mathrm{T}}^{n/3}$ is observed for all flow harmonics at low p_{T} $(0.2 < p_{\mathrm{T}} < 3\,\mathrm{GeV}/c)$. At the same time, the ratios $v_n/v_m^{n/m}$ are observed to be essentially independent of p_{T} for most centralities up to about $p_{\mathrm{T}} = 10\,\mathrm{GeV}/c$. Analysing the differences among higher-order cumulants of elliptic flow (v_2), which have different sensitivities to flow fluctuations, a measurement of the standardised skewness of the event-by-event v_2 distribution $P(v_2)$ is reported and constraints on its higher moments are provided. The Elliptic Power distribution is used to parametrise $P(v_2)$, extracting its parameters from fits to cumulants. The measurements are compared to different model predictions in order to discriminate among initial-state models and to constrain the temperature dependence of the shear viscosity to entropy-density ratio.

Contents

1 Introduction

The primary goal of ultra-relativistic heavy-ion collisions is to study the properties of QCD matter at extremely high temperatures and/or densities and to understand the microscopic dynamics from which these properties arise, especially in the non-perturbative regime. The study of anisotropies in the azimuthal distribution of produced particles, commonly called anisotropic flow, has contributed significantly to the characterization of the system created in heavy-ion collisions [1–5]. According to the current paradigm of bulk particle production, anisotropic flow is determined by the response of the system to its initial spatial anisotropies. Initial-state spatial anisotropies come in turn from both the geometry of the collision and fluctuations in the wave function of the incident nuclei [3–8]. The significant magnitude of anisotropic flow is interpreted as evidence of the formation of a strongly-coupled system, which can effectively be described as a fluid with very low shear viscosity to entropy-density ratio (η/s) [9].

Anisotropic flow is quantified by the coefficients v_n of a Fourier series decomposition of the distribution in azimuthal angle φ of final-state particles [10]

$$\frac{\mathrm{d}N}{\mathrm{d}\varphi} \propto 1 + 2 \sum_{n=1}^{+\infty} v_n \cos\left[n(\varphi - \Psi_n)\right], \tag{1.1}$$

where Ψ_n corresponds to the symmetry plane angle of order n. The dominant flow coefficient in non-central heavy-ion collisions is the second flow harmonic (v_2), called elliptic flow, which is mostly a result of the average ellipsoidal shape of the overlapping area between the colliding nuclei, whereas higher harmonics originate from initial-state fluctuations. For transverse momenta $p_\mathrm{T} \lesssim 3\,\mathrm{GeV}/c$, anisotropic flow is thought to be quantitatively determined by the whole evolution of the system, including the phase of hadronic rescatterings

that takes place after chemical freeze-out [11]. Flow coefficients have been shown to be sensitive not only to initial-state anisotropies, but also to the transport parameters (such as shear and bulk viscosity [12, 13]) and the equation of state of the system, and they have therefore been used to constrain these properties [14, 15]. However, given the different heterogeneous phases that the system is believed to undergo, it has not been possible so far to simultaneously constrain the large number of model parameters, although attempts have been made [16, 17].

In this regard, the energy dependence of anisotropic flow has been shown to provide additional discriminating power over initial-state models and temperature dependence of transport parameters [18, 19]. In fact, some theoretical uncertainties in the determination of anisotropic flow coefficients are expected to partially cancel in the ratios of v_n coefficients measured at different collision energies, such as those on the choice of initial-state model or on the absolute value of η/s. These ratios would then effectively constrain the variations with collision energy and, therefore, system temperature of the parameters to which anisotropic flow is most sensitive.

It is known that the magnitude of anisotropic flow, being approximately proportional to the initial-state spatial anisotropy [20], fluctuates from collision to collision even for fixed centrality [6, 21–24], and that its probability distribution function (p.d.f.) $P(v_n)$ is to a first approximation Bessel-Gaussian [1, 25], i.e. the product of a modified Bessel function and a Gaussian function. It has been pointed out that small deviations from a Bessel-Gaussian shape are to be expected independently from the details of initial-state fluctuations [26–28]. Evidence of such small deviations has been previously reported [29]. These deviations are due to first order to the flow p.d.f. having a finite skewness. Its quantitative determination would therefore improve the characterization of these deviations. For dimensional reasons, it is convenient to use a standardised skewness (γ_1), defined as [30]

$$\gamma_1 = \frac{\langle (v_n\{\mathrm{RP}\} - \langle v_n\{\mathrm{RP}\}\rangle)^3 \rangle}{\langle (v_n\{\mathrm{RP}\} - \langle v_n\{\mathrm{RP}\}\rangle)^2 \rangle^{3/2}}, \tag{1.2}$$

where $v_n\{\mathrm{RP}\}$ refers to the anisotropic flow with respect to the reaction plane Ψ_{RP}, i.e. the plane spanned by the impact parameter and the beam axis, and the brackets $\langle \cdots \rangle$ indicate an average over all events. It is worthwhile to note that the symmetry planes Ψ_n do not generally coincide with Ψ_{RP} because of initial-state fluctuations.

A robust experimental method to quantify flow fluctuations is to measure v_n with multi-particle cumulants, which have different sensitivities to the moments of the underlying flow p.d.f. $P(v_n)$

$$v_n\{2\} = \sqrt[2]{\langle v_n^2 \rangle}, \tag{1.3}$$

$$v_n\{4\} = \sqrt[4]{2\langle v_n^2 \rangle^2 - \langle v_n^4 \rangle}, \tag{1.4}$$

$$v_n\{6\} = \sqrt[6]{\langle v_n^6 \rangle - 9\langle v_n^2 \rangle\langle v_n^4 \rangle + 12\langle v_n^2 \rangle^3}, \tag{1.5}$$

$$v_n\{8\} = \sqrt[8]{\langle v_n^8 \rangle - 16\langle v_n^2 \rangle\langle v_n^6 \rangle - 18\langle v_n^4 \rangle^2 + 144\langle v_n^2 \rangle^2\langle v_n^4 \rangle - 144\langle v_n^2 \rangle^4}. \tag{1.6}$$

The number in curly brackets indicates the order of the cumulant.

For elliptic flow, a large difference between $v_2\{2\}$ and $v_2\{4\}$ and approximately equal values of the higher order cumulants ($v_2\{4\}$, $v_2\{6\}$, $v_2\{8\}$) have been previously observed [29, 31], which is indeed consistent with an approximately Bessel-Gaussian flow p.d.f.. However, a fine-splitting of a few percent among the higher order cumulants ($v_2\{4\}$, $v_2\{6\}$, $v_2\{8\}$) has also been reported [29], which is thought to be determined by the residual deviations from Bessel-Gaussian shape, in particular a non-zero skewness. A negative value of γ_1, which corresponds to $P(v_2)$ being left skewed, is expected [27] from the necessary condition on the initial-state eccentricity $\varepsilon_2 < 1$, which acts as a right cutoff on $P(v_2)$. The Elliptic Power distribution, proposed in [26, 27], was motivated mainly by this observation and it was shown to provide a good description of $P(v_2)$ in a wide centrality range [32]. Moreover, γ_1 has been predicted to increase in absolute value from central to peripheral collisions [30], being roughly proportional to $\langle v_2\{\mathrm{RP}\}\rangle$ and being inversely proportional to the square root of the system size [28]. γ_1 can be estimated from the fine-splitting among two- and multi-particle cumulants [30]

$$\gamma_1^{\mathrm{exp}} = -6\sqrt{2}v_2\{4\}^2 \frac{v_2\{4\} - v_2\{6\}}{(v_2\{2\}^2 - v_2\{4\}^2)^{3/2}}. \tag{1.7}$$

It is denoted as γ_1^{exp} to emphasize that it does not exactly match the definition of γ_1 given in eq. (1.2), although the two have been estimated to coincide within a few percents [30]. The derivation of eq. (1.7) relies on a Taylor expansion of the generating function in powers of the moments, truncated at the order of the skewness. It is experimentally possible to test the validity of this approximation through the universal equality that it implies [30, 33]

$$v_2\{6\} - v_2\{8\} = \frac{1}{11}(v_2\{4\} - v_2\{6\}). \tag{1.8}$$

The precision up to which this equality holds depends on the residual contribution of higher central moments of the flow p.d.f., e.g. the kurtosis, to the multi-particle cumulants.

At high p_{T} ($p_{\mathrm{T}} \gtrsim 10\,\mathrm{GeV}/c$) the dominant mechanism that determines azimuthal anisotropies of the produced final-state particles is thought to be path-length dependent energy-loss of highly energetic partons [34–36]. Although several experimental observations, such as jet azimuthal anisotropies [37, 38], are consistent with this hypothesis, the details of the process are largely unconstrained and measurements of anisotropic flow of high-p_{T} particles can help in this regard. Although the mechanism that determines it is fundamentally different, the origin of anisotropic flow at high p_{T} is common to the one at low p_{T}: initial-state geometry and its event-by-event fluctuations. Measurements reported in [39] seem to confirm this interpretation.

Recent CMS results on non-Gaussian elliptic flow fluctuations [40] appeared during the writing of this article. Numerical data are not yet available, but the observations seem to be essentially compatible with our measurements and their conclusions agree with those of this article.

2 Data sample and analysis methods

The sample of Pb–Pb collisions used for this measurement was recorded with the ALICE detector [41, 42] in November and December 2015 (2010), during the Run 2 (Run 1) of the

LHC, at a centre of mass energy per nucleon of $\sqrt{s_{NN}} = 5.02\,(2.76)$ TeV. The detectors used in the present analysis are the Inner Tracking System (ITS) and Time Projection Chamber (TPC), for primary vertex determination and charged particle tracking, and the V0 detector, for symmetry plane determination, centrality estimation [43] and trigger. The trigger conditions are described in [41]. About $78.4 \times 10^6\,(12.6 \times 10^6)$ minimum-bias events in the centrality range 0–80%, corresponding to an integrated luminosity of 12.7 μb^{-1} (2.0 μb^{-1}), with a reconstructed primary vertex position along the beam direction (z_{vtx}) within ± 10 cm from the nominal interaction point, passed offline selection criteria [41] for the data sample at $\sqrt{s_{NN}} = 5.02\,(2.76)$ TeV. Centrality is determined from the measured amplitude in the V0, which is proportional to the number of charged tracks in the corresponding acceptance ($2.8 < \eta < 5.1$ for V0A and $-3.6 < \eta < -1.7$ for V0C).

Charged tracks with transverse momentum $0.2 < p_{\text{T}} < 50\,\text{GeV}/c$ and pseudorapidity $|\eta| < 0.8$ are used in the present analysis. These tracks are reconstructed using combined information from the ITS and TPC. A minimum number of TPC space points of 70 (out of 159) is required for all tracks, together with a χ^2 per TPC space point (χ^2_{TPC}) in the range $0.1 < \chi^2_{\text{TPC}} < 4$. A minimum number of 2 ITS hits, of which at least one in the two innermost layers, is required, together with a χ^2 per ITS hit per degree of freedom (χ^2_{ITS}) smaller than 36. Only tracks with a distance of closest approach (DCA) to the primary vertex position less than 3.2 cm in the beam direction and 2.4 cm transverse to it are used. These track selection criteria ensure an optimum rejection of secondary particles and a p_{T} resolution better than 5% in the p_{T} range used in the present analysis [41].

Anisotropic flow coefficients are measured with the Q-cumulant method [44], using the implementation proposed in [45]. Track weights (w) are used in the construction of the Q-vectors, in order to correct for non-uniform reconstruction efficiency and acceptance

$$Q_{n,m} = \sum_{j=1}^{M} w_j(p_{\text{T}}, \eta, \varphi, z_{\text{vtx}})^m e^{in\varphi_j}, \tag{2.1}$$

where M is the charged track multiplicity, n the harmonic and m an integer exponent of the weights. After applying track weights, the effects due to non-uniformities in azimuthal acceptance, which would introduce a bias in the measured flow coefficients, are observed to be negligible. This is evaluated by measuring the event-averaged values of the real and imaginary part of Q_n, which are consistent with zero. Multi-particle cumulants are measured on an event-by-event basis and then, in order to minimise statistical fluctuations, averaged over all events using the corrected charged track multiplicity as a weight, following the procedure proposed in [44]. All observables are computed in small centrality bins (1%) and then integrated, when limited size of the data sample makes it necessary, in wider centrality intervals using the charged particle yield in each 1% centrality bin as weight. This avoids that the event weighting procedure, based on multiplicity, would introduce a bias in the average centrality within a large centrality bin, since multiplicity varies with centrality.

For p_{T}-integrated results, the m-particle cumulants are calculated using all tracks within given p_{T} range, while for p_{T}-differential results one particle at a given p_{T} is correlated with $m - 1$ particles in the full p_{T} range ($0.2 < p_{\text{T}} < 50\,\text{GeV}/c$). In terms of reference

$(c_n\{m\})$ and differential $(d_n\{m\})$ cumulants, as defined in [44], the flow coefficients are measured as

$$v_n\{2\} = \sqrt[2]{c_n\{2\}}, \tag{2.2}$$

$$v_n\{4\} = \sqrt[4]{-c_n\{4\}}, \tag{2.3}$$

$$v_n\{6\} = \sqrt[6]{\frac{1}{4}c_n\{6\}}, \tag{2.4}$$

$$v_n\{8\} = \sqrt[8]{-\frac{1}{33}c_n\{8\}}, \tag{2.5}$$

$$v_n\{2\}(p_{\mathrm{T}}) = d_n\{2\}(p_{\mathrm{T}})/\sqrt[2]{c_n\{2\}}, \tag{2.6}$$

$$v_n\{4\}(p_{\mathrm{T}}) = -d_n\{4\}(p_{\mathrm{T}})/\sqrt[4]{-c_n\{4\}^3}. \tag{2.7}$$

For two-particle correlations, a separation in pseudorapidity between the correlated particles $(\Delta\eta)$ is applied in order to suppress short-range azimuthal correlations which are not associated to the symmetry planes, usually called 'non-flow'. These correlations arise from jets, mini-jets and resonance decays. For flow coefficients of higher order $(v_n\{m > 2\})$, non-flow contribution has been previously found to be negligible in Pb–Pb collisions [24, 31]. Results corresponding to $|\Delta\eta| > 1$ (denoted with $v_n\{2, |\Delta\eta| > 1\}$) are obtained with the two-particle cumulant correlating tracks from opposite sides of the TPC acceptance, $-0.8 < \eta < -0.5$ and $0.5 < \eta < 0.8$. Results corresponding to $|\Delta\eta| > 2$ (and reported as $v_n\{2, |\Delta\eta| > 2\}$) are obtained with the scalar product method [46], correlating all tracks at mid-rapidity $(|\eta| < 0.8)$ with the n-th harmonic Q-vector Q_n^{V0A} calculated from the azimuthal distribution of the energy deposition measured in the V0A detector [2, 47]

$$v_n\{2, |\Delta\eta| > 2\} = \frac{\langle u_{n,0} Q_n^{\mathrm{V0A}*} \rangle}{\sqrt{\frac{\langle Q_n^{\mathrm{V0A}} Q_{n,1}^* \rangle \langle Q_n^{\mathrm{V0A}} Q_n^{\mathrm{V0C}*} \rangle}{\langle Q_{n,1} Q_n^{\mathrm{V0C}*} \rangle}}}, \tag{2.8}$$

where $u_{n,0} = e^{in\varphi}$ is the unit flow vector from charged particle tracks at mid-rapidity and $Q_{n,1}$ is computed from the same type of tracks according to eq. (2.1). Both methods have their own limitations and thus are complementary to each other: $v_n\{2, |\Delta\eta| > 2\}$ can be reliably employed only up to the fourth harmonic, because of the finite azimuthal segmentation of the V0 detectors (8 sectors in 2π), while $v_n\{2, |\Delta\eta| > 1\}$ suffers from bigger statistical uncertainties, due to the limited acceptance from which tracks are selected, and bigger non-flow contribution for $p_{\mathrm{T}} > 10\,\mathrm{GeV}/c$.

The systematic uncertainties are evaluated by varying the track and event selection criteria and comparing the variation in the flow coefficients relative to the default results. The absolute value of the variation itself is assigned as a systematic uncertainty if it is considered significant according to the Barlow criterion [48]. Different track quality variables are varied: number of TPC space points, χ^2_{TPC} and χ^2_{ITS}, fraction of shared TPC space points and number of ITS hits. For each of these, the default values are varied in order to increase the fraction of excluded tracks as much as 5 times. No significant differences are observed in the reported measurements between positively and negatively charged particles. Concerning the event selection criteria, the following are investigated: polarity of the
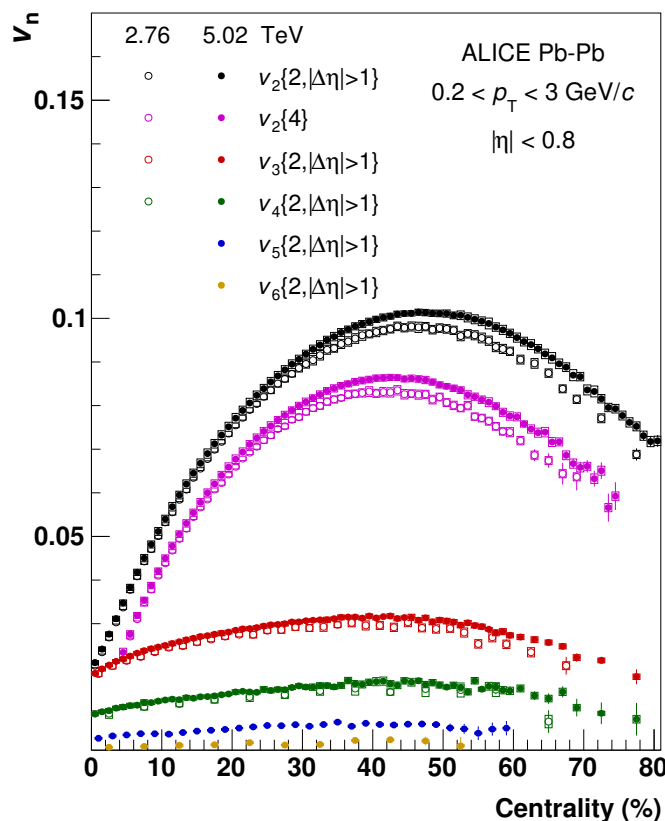
Figure 1. Anisotropic flow coefficients v_n of inclusive charged particles as a function of centrality, for the two-particle (denoted with $|\Delta\eta| > 1$) and four-particle cumulant methods. Measurements for Pb–Pb collisions at $\sqrt{s_{\mathrm{NN}}} = 5.02$ (2.76) TeV are shown by solid (open) markers.

magnetic field, reconstructed primary vertex position along the beam direction (selecting only events with z_{vtx} within ± 8 cm from the nominal interaction point), pile-up rejection (imposing stronger or weaker constraints on the consistency of different event multiplicity estimators) and variations in the instantaneous luminosity delivered to the ALICE detector by the LHC. The uncertainty on centrality determination is evaluated using an alternative estimator based on the number of hits in the second ITS layer ($|\eta| < 1.4$), which is directly proportional to the number of charged particles in the corresponding acceptance. Among the aforementioned sources, for all observables in this article, track quality and centrality determination are the dominant sources. The total systematic uncertainties are evaluated summing in quadrature the systematic uncertainties coming from each of the sources, i.e. considering the different sources to be uncorrelated.

3 Collision energy, transverse momentum and centrality dependence

Figure 2 shows the ratio of $v_n\{2, |\Delta\eta| > 1\}$ ($n = 2, 3, 4$) and $v_2\{4\}$ between $\sqrt{s_{\mathrm{NN}}} = 5.02$ and 2.76 TeV, i.e. the relative variation of these flow coefficients between those two energies. Since the systematic uncertainties of the measurements at different energies are partially

	$\eta/s = 0.2$	$\eta/s(T)$ param1	1
$v_2\{2, |\Delta\eta| > 1\}$	0.712	0.645	0.477
$v_2\{4\}$	0.467	0.357	0.028
$v_3\{2, |\Delta\eta| > 1\}$	0.053	0.003	0.001
$v_4\{2, |\Delta\eta| > 1\}$	0.484	0.468	0.022

Table 1. p-values for the comparison among ratios of $v_n\{2, |\Delta\eta| > 1\}$ ($n = 2, 3, 4$) and $v_2\{4\}$ between $\sqrt{s_{NN}} = 5.02$ and $2.76\,\mathrm{TeV}$ and model calculations using different parametrisations of $\eta/s(T)$ [18], shown in figure 2, and unity, in the centrality range 5-50%.

correlated, the resulting systematic uncertainty on the ratio is reduced. All harmonics are observed to increase with energy, between about 2 and 10%. A hint of a centrality dependence is observed only for v_2, with the increase growing slightly from mid-central towards more peripheral collisions. No significant difference is observed in the increase of v_2 measured with two- or four-particle correlations. Since the difference between $v_2\{2, |\Delta\eta| > 1\}$ and $v_2\{4\}$ is directly related to flow fluctuations, this observation suggests that the fluctuations of elliptic flow do not vary significantly between the two energies, within experimental uncertainties. The ratios are compared to hydrodynamical calculations with EKRT initial conditions [51] and different parametrisations of the temperature dependence of η/s [18]. The p-values for the comparison between data and models are also shown in Tab. 1. Among the two parametrisations that provide the best description of RHIC and LHC data [52], both are consistent with the measurements, except for $v_3\{2, |\Delta\eta| > 1\}$, albeit the one with constant $\eta/s = 0.2$ agrees slightly better. These comparisons take into account the correlation between systematic uncertainties of data points in different centrality intervals. This observation might indicate little or no temperature dependence of η/s within the temperature range at which anisotropic flow develops at the two center of mass energies. As a reference, the p-values for the comparison between data and unity in the same centrality range (5–50%) are also reported in table 1.

Looking at the p_T dependence in more detail, the flow harmonics are found to follow an approximate power-law scaling up to around the maximum, with exponents being proportional to the harmonic number n, $v_n(p_T) \sim p_T^{n/3}$, as shown by the dashed fitted lines in figure 3. In ideal hydrodynamics, the p_T dependence of anisotropic flow for massive particles should follow a power-law function $v_n(p_T) \sim p_T^n$ in the region of p_T/M up to order one, where M is the particle's mass, and at higher momenta it has been predicted to be linear in p_T for all n, $v_n(p_T) \sim p_T$ [53, 54]. This p_T dependence is notably different from the one observed in the data. At very low p_T this is presumably because the relevant momentum region for inclusive particles, mostly pions, is below the range of our measurements, and at higher p_T ideal hydro is not expected to hold because of momentum dependent viscous corrections at freeze out [55] and/or non-linear mode mixing for $n \geqslant 4$ [20, 56]. The power-law dependence for $n = 2$ was noticed before and it was attributed to a novel energy loss mechanism [57], which however cannot explain the scaling observed for $n > 2$. The emergence of this simple power-law dependence remains unexpected and surprising.
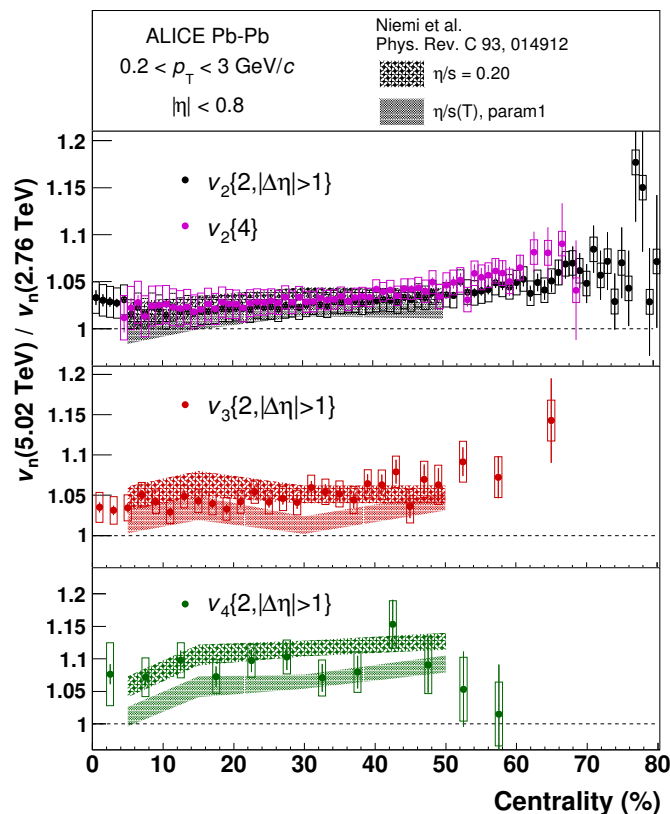
Figure 2. Ratios of anisotropic flow coefficients v_n of inclusive charged particles between Pb–Pb collisions at $\sqrt{s_{\mathrm{NN}}} = 5.02$ and $2.76\,\mathrm{TeV}$, as a function of centrality. Hydrodynamic calculations employing different $\eta/s(T)$ parametrizations [18] are shown for comparison.

Figure 4 shows the p_{T}-differential measurements of v_n ($n = 2, 3, 4$) calculated with the scalar product method with respect to V0A. The same p_{T} and centrality range as in figure 3 is shown. A significant $v_2\{2, |\Delta\eta| > 2\}$ is observed up to $p_{\mathrm{T}} \approx 40\,\mathrm{GeV}/c$ in the centrality range 10–40%. $v_n\{2, |\Delta\eta| > 2\}$ and $v_n\{2, |\Delta\eta| > 1\}$ ($n = 2, 3, 4$) are found to be compatible within 2% in the p_{T} range $0.2 < p_{\mathrm{T}} < 10\,\mathrm{GeV}/c$, while a systematic difference (with $v_2\{2, |\Delta\eta| > 1\} > v_2\{2, |\Delta\eta| > 2\}$) is observed for $10 < p_{\mathrm{T}} < 50\,\mathrm{GeV}/c$, ranging from about 3% in centrality 0–5% to about 10% in centrality 40–50%. This difference is attributed to small residual non-flow contributions which are suppressed by the larger pseudorapidity gap. Two-particle non-flow contributions roughly scale as the inverse of the multiplicity [2], which is consistent with the observed centrality dependence. Possible differences among $v_n\{2, |\Delta\eta| > 1\}$ and $v_n\{2, |\Delta\eta| > 2\}$ ($n = 2, 3, 4$) arising from the decorrelation of event planes at different pseudorapidities have been estimated to be less than 1% and 3% for v_2 and v_{3-4}, respectively, based on η-dependent factorization ratios [58] measured at $2.76\,\mathrm{TeV}$ [59]. This estimation assumes that such decorrelation only depends on $|\Delta\eta|$ and not η in the pseudorapidity range under consideration ($|\eta| < 5.1$).

Figure 5 shows the ratios of p_{T}-differential $v_n\{2, |\Delta\eta| > 1\}$ ($n = 2, 3, 4$) and $v_2\{4\}$ between $\sqrt{s_{\mathrm{NN}}} = 5.02$ and $2.76\,\mathrm{TeV}$. Overall, the ratios are consistent with unity, indicating
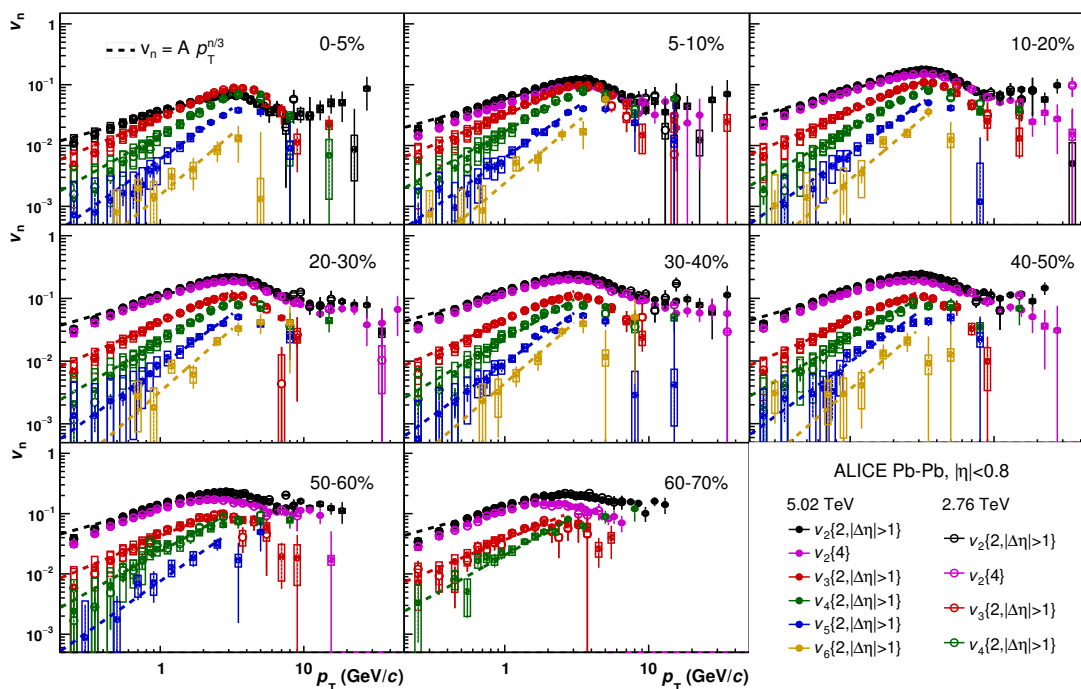
Figure 3. Anisotropic flow coefficients $v_n(p_T)$ of inclusive charged particles in different centrality classes, measured with two-particle (denoted with $|\Delta\eta| > 1$) and four-particle cumulant methods. Measurements for Pb–Pb collisions at $\sqrt{s_{NN}} = 5.02$ (2.76) TeV are shown by solid (open) markers. Dashed lines are fits with a power-law function $v_n(p_T) = A\,p_T^{n/3}$, with A as free parameter.

that p_T-differential anisotropic flow does not change significantly across collision energies and that the increase observed in the p_T-integrated values can be mostly attributed to an increase of $\langle p_T \rangle$, as previously noted [49]. This observation is also consistent with little or no variation of η/s between the two collision energies, as already shown in figure 2. The possible variations in p_T-integrated values arising from the differences in the p_T-differential ones have been estimated to be less than 1%, by integrating $v_n(p_T)$ at $\sqrt{s_{NN}} = 5.02$ (2.76) TeV with charged particle spectra at 2.76 (5.02) TeV.

Figure 6 shows the comparison of p_T-differential flow measurements with different models, in three centrality intervals: 5–10% (top panel), 20–30% (middle panel) and 40–50% (bottom panel). At low p_T ($p_T < 2\,\text{GeV}/c$), flow coefficients are expected to be mostly determined by the collective expansion of the system, which is commonly described by hydrodynamic models. The measurements are compared to three calculations, one employing IP-Glasma initial conditions [60] matched to the MUSIC viscous hydrodynamic code [61] and two calculations using iEBE-VISHNU viscous hydrodynamic code [62] with AMPT [63] or TRENTo [64] initial conditions. The parameters of TRENTo were tuned to reproduce previous measurements in Pb–Pb collisions at $\sqrt{s_{NN}} = 2.76\,\text{TeV}$ [16]; with such tuning TRENTo has been shown [64] to effectively mimic IP-Glasma initial conditions and therefore the two calculations TRENTo+iEBE-VISHNU and IP-Glasma+MUSIC are expected to be based on similar initial conditions. All models employ a transport cascade
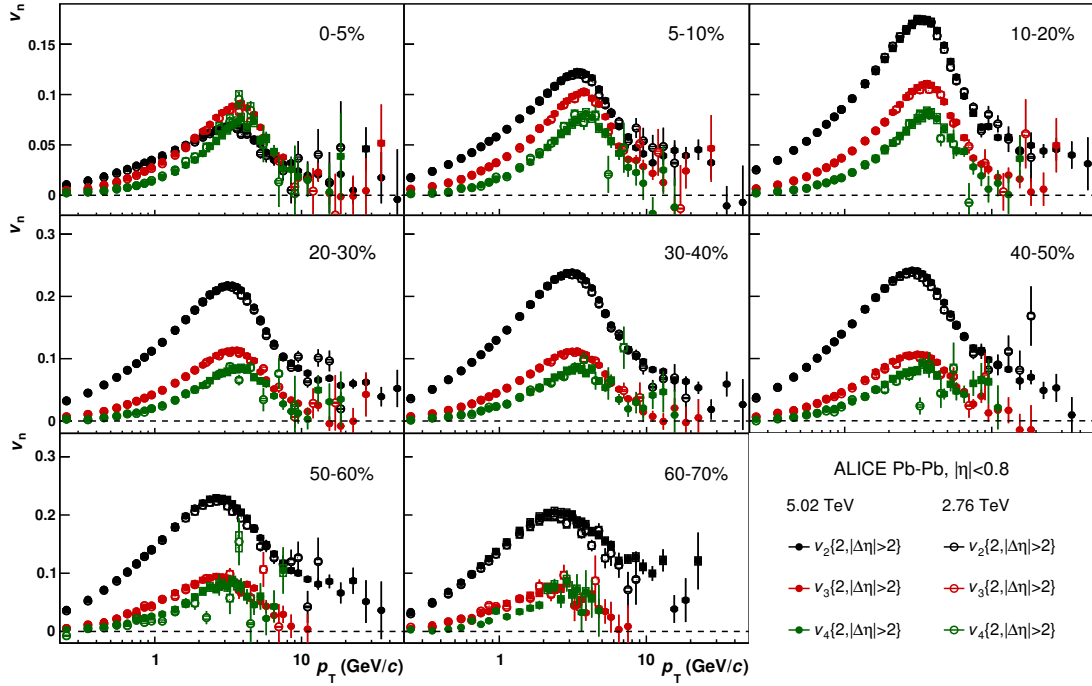
Figure 4. Anisotropic flow coefficients $v_n(p_T)$ of inclusive charged particles in different centrality classes, measured with the scalar product method with respect to the V0A Q-vector. Measurements for Pb–Pb collisions at $\sqrt{s_{NN}} = 5.02$ (2.76) TeV are shown by solid (open) markers.
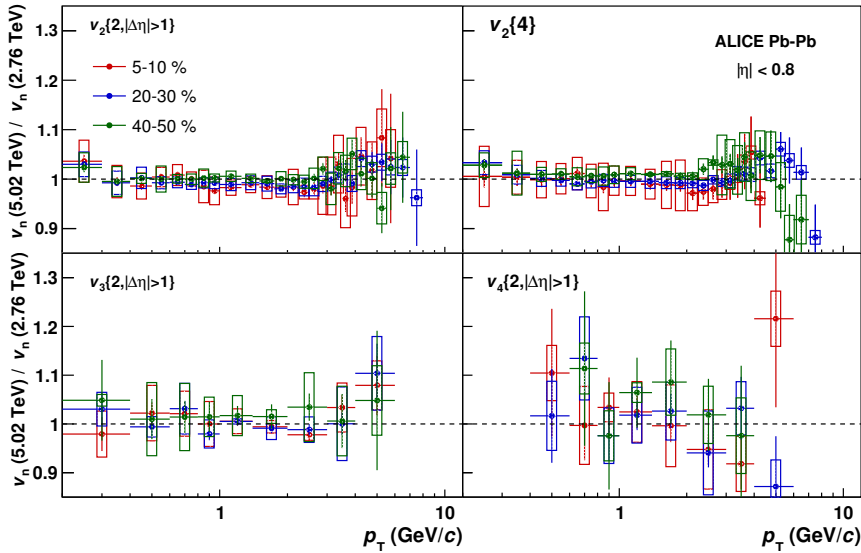

Figure 5. Ratios of anisotropic flow coefficients $v_n(p_T)$ of inclusive charged particles between Pb–Pb collisions at $\sqrt{s_{NN}} = 5.02$ and 2.76 TeV, in different centrality classes, measured with two-particle (denoted with $|\Delta\eta| > 1$) and four-particle cumulant methods.

model (UrQMD [65]) to describe the hadronic phase after freeze-out. Compared to data, all models are found to underestimate the data for $p_T < 0.5\,\mathrm{GeV}/c$. For $1 < p_T < 2\,\mathrm{GeV}/c$ the predictions from IP-Glasma+MUSIC and TRENTo+iEBE-VISHNU overestimate the data, while those from AMPT-IC+iEBE-VISHNU are found to be still in agreement. Overall, all models qualitatively describe the p_T dependence of flow coefficients in this low p_T range.

At high p_T ($p_T > 10\,\mathrm{GeV}/c$), azimuthal anisotropies are on the contrary expected to be determined by path-length dependent parton energy-loss. The measurements are compared to predictions from [66], which combine an event-by-event hydrodynamic description of the medium (v-USPhydro [67]) with a jet quenching model (BBMG [68]). Two sets of predictions for $v_2\{2\}$, $v_2\{4\}$ and $v_3\{2\}$, assuming a linear ($\mathrm{d}E/\mathrm{d}x \sim L$) and a quadratic ($\mathrm{d}E/\mathrm{d}x \sim L^2$) dependence of the energy loss on the path length L, are compared to data. Other parameters of the model, such as η/s, are expected to have a minor contribution within the presented centrality ranges [66]. For $v_2\{2, |\Delta\eta| > 2\}$, the linear case is compatible with the data, while the quadratic one can be excluded within 95% confidence level. For $v_3\{2, |\Delta\eta| > 2\}$, neither of the two sets of predictions can be excluded within uncertainties. Our results are found to be in good agreement with CMS data [39].

The evolution of the shape of p_T-differential v_n coefficients with respect to centrality is investigated by calculating the ratios of $v_n(p_T)$ in a given centrality range and $v_n(p_T)$ in centrality 20–30%, normalised by the corresponding ratio of p_T-integrated v_n

$$v_n(p_T)_{\text{ratio to 20-30\%}} = \frac{v_n(p_T)}{v_n(p_T)[\text{20-30\%}]} \frac{v_n[\text{20-30\%}]}{v_n}. \tag{3.1}$$

In order to reduce statistical fluctuations, a parametrisation of $v_n(p_T)[\text{20-30\%}]$ fitted to data is employed. If the shape of $v_n(p_T)$ does not change with centrality, $v_n(p_T)_{\text{ratio to 20-30\%}}$ is identical to 1 in the full p_T range. The results are shown in figure 7: deviations from unity up to about 10% are observed at low p_T ($p_T < 3\,\mathrm{GeV}/c$) and up to about 30% at intermediate p_T ($3 < p_T < 6\,\mathrm{GeV}/c$), where $v_n(p_T)$ reaches its maximum. These variations are observed to be larger for higher harmonics (v_{3-4}), in particular for central collisions. The effects due to a change in particle composition of the inclusive charged particle sample with centrality are estimated to be negligible. These deviations are attributed mostly to the combined effect of radial flow and parton density which, in the coalescence model picture [69], decrease from central to peripheral collision shifting the maximum of $v_n(p_T)$ from higher to lower p_T. At high p_T ($p_T > 10\,\mathrm{GeV}/c$), results on $v_2\{2, |\Delta\eta| > 2\}$ are consistent with those at low p_T, suggesting a common origin of the centrality evolution of elliptic flow in the two regimes, presumably initial-state geometry and its fluctuations. This interpretation is consistent with the findings of [39]. The attribution of the scaling of $v_n(p_T)$ up to $p_T = 8\,\mathrm{GeV}/c$ to initial-state geometries agrees with studies [70, 71] using the Event Shape Engineering technique [72] and p_T-dependent elliptic flow fluctuations [73]. Finally, the models using hydrodynamic calculations [62] and jet energy loss ones [66] are observed to be in good agreement with the v_2 data at low and high p_T, respectively.

At RHIC [74, 75] and LHC [7] it had been observed that the ratios of harmonics follow a power-law scaling, i.e. $v_n^{1/n} \sim v_m^{1/m}$, for semi-central and peripheral collisions up to about $6\,\mathrm{GeV}/c$ and independent of the harmonic n and m. In order to test this scaling, we
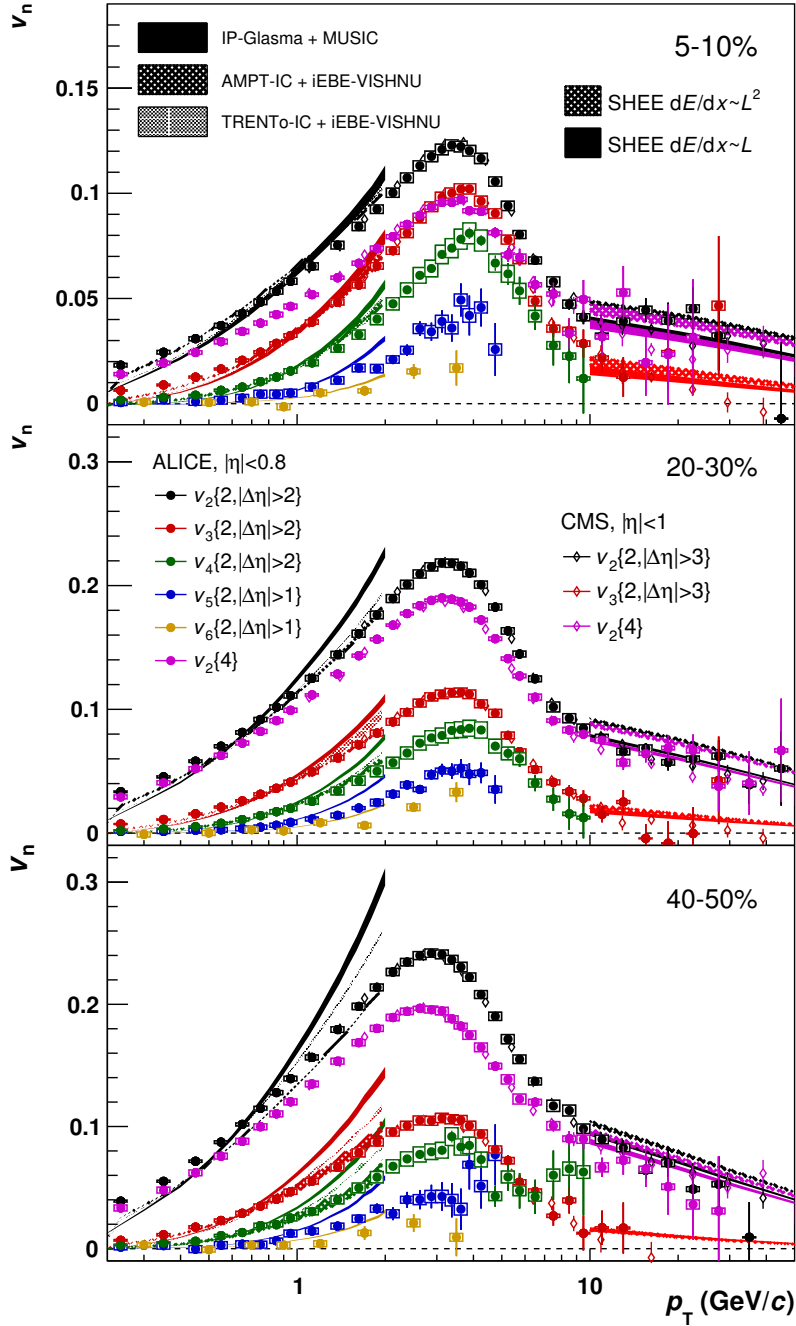
Figure 6. Anisotropic flow coefficients $v_n(p_T)$ of inclusive charged particles in different centrality classes, measured with two- and four-particle cumulant and scalar product methods with respect to the V0A Q-vector, for Pb–Pb collisions at $\sqrt{s_{NN}} = 5.02$ TeV. Several hydrodynamic calculations [61, 62, 66] and previous measurements from CMS [39] are shown for comparison.
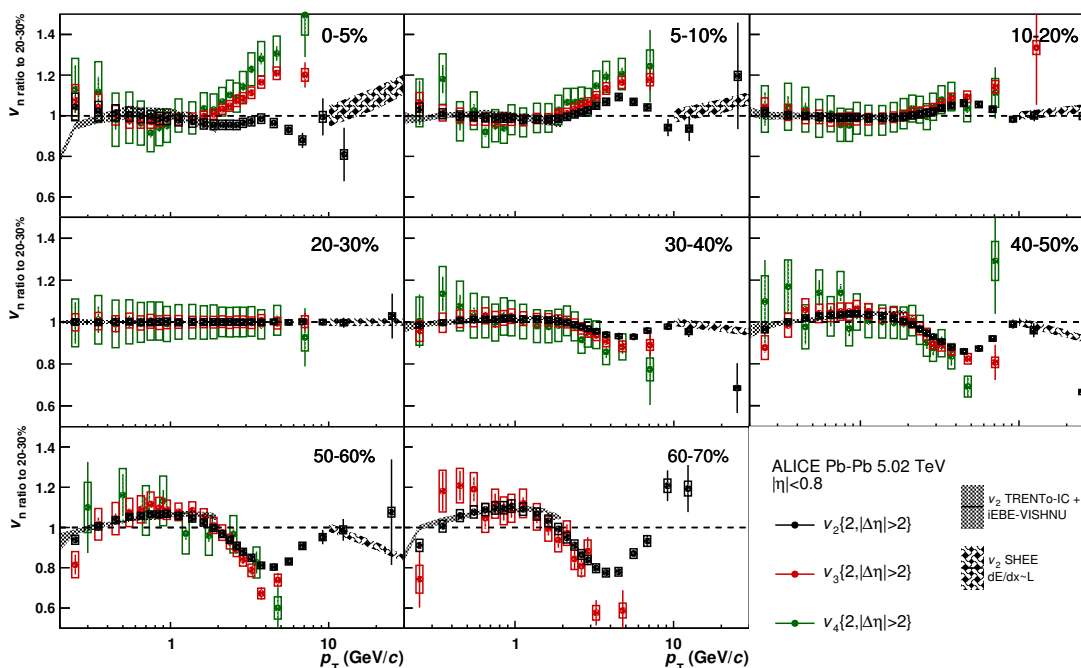
Figure 7. Ratios $v_n(p_T)_{\text{ratio to 20-30\%}}$ of inclusive charged particles for Pb–Pb collisions at $\sqrt{s_{NN}} = 5.02\,\text{TeV}$, in different centrality classes, measured with the scalar product method with respect to the V0A Q-vector. Hydrodynamic calculations [62, 66] are shown for comparison.

use the ratios $v_n/v_m^{n/m}$ which in practice are more sensitive than $v_n^{1/n} \sim v_m^{1/m}$. Figure 8 shows these ratios for $n = 3, 4$ and $m = 2, 3$, as a function of p_T. These ratios are indeed observed to be independent of p_T, in most of the p_T range and for most centrality ranges, except for centrality 0–5%. Up to about the maximum of $v_n(p_T)$, the scaling is numerically related to, but actually significantly more precise than, the observed approximate power-law dependences $v_n(p_T) \sim p_T^{n/3}$ pointed out in figure 3. Surprisingly however, the scaling extends much further, in particular $v_3(p_T)/v_2(p_T)^{3/2}$ is constant to better than about 10%, out to the highest measured p_T in excess of $10\,\text{GeV}/c$. The ratio $v_4(p_T)/v_2(p_T)^{4/2}$ shows stronger deviations at high p_T, starting at around the maximum of $v_2(p_T)$. A separation of v_4 into linear and non-linear components would be required to see if the v_4/v_2 scaling at low p_T, and/or its violations at high p_T, is related to the mode mixing, which is particularly strong for the 4th harmonic and at high p_T, or possibly also to quark coalescence [53, 76, 77].

As noted in the context of figure 3, the observed ratio scaling is not expected in ideal hydrodynamics. While not all viscous hydrodynamical models shown in figure 6 describe the data up to the highest p_T very well, they all do exhibit the same power-law scaling in the ratio of harmonics over the p_T range $0.5 < p_T < 3\,\text{GeV}/c$, with a precision comparable to the one seen in the data, while they strongly deviate for $p_T < 0.5\,\text{GeV}/c$. The scaling may be related to viscosity, as also postulated in [78, 79], in particular to the large and p_T-dependent viscous corrections appearing at hadronisation [55]. However, a harmonic number dependence of these viscous corrections which could reproduce the scaling observed in the data, has so far, to the best of our knowledge, never been quantitatively investigated.
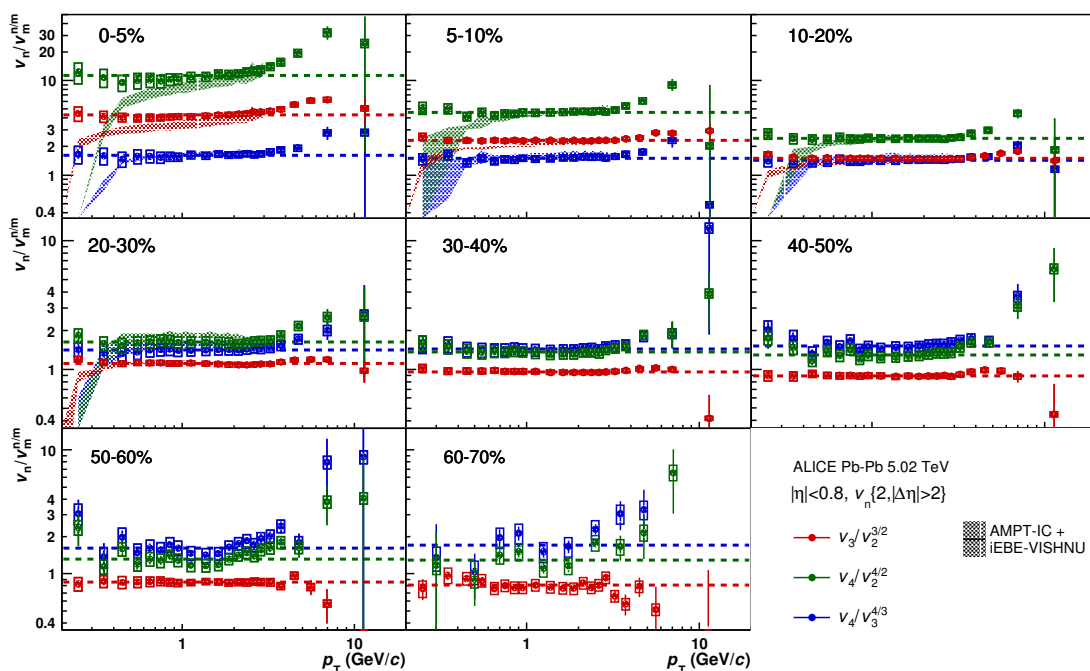
Figure 8. Ratios $v_n(p_T)/v_m(p_T)^{n/m}$, $n = 3, 4$, $m = 2, 3$ of inclusive charged particles for Pb–Pb collisions at $\sqrt{s_{NN}} = 5.02$, in different centrality classes, measured with the scalar product method with respect to the V0A Q-vector. Dashed lines represent averages in $0.2 < p_T < 3\,\mathrm{GeV}/c$. The ratios are also shown for one hydrodynamic model [62] in the four most central centrality intervals; it is qualitatively similar in the other centrality intervals and for the other models.

4 Elliptic flow fluctuations

Figure 9 shows the integrated v_2 in the p_T range $0.2 < p_T < 3\,\mathrm{GeV}/c$ as a function of centrality, measured with two-, four-, six- and eight-particle cumulants at $\sqrt{s_{NN}} = 5.02$ and $2.76\,\mathrm{TeV}$. The corresponding cumulants ($c_2\{2, 4, 6, 8\}$) are reported in figure 10. The centrality dependence is similar for all multi-particle cumulants and similar to what is shown in figure 1. The differences between $v_2\{2\}$ (shown in figure 9) and $v_2\{2, |\Delta\eta| > 1\}$ (shown in figure 1), which range from about 4% in mid-central collisions to about 20% in peripheral ones, are mostly attributed to non-flow contributions, which are suppressed in the case of results with a pseudorapidity gap. The possible differences arising from the decorrelation of event planes at different pseudorapidities are expected to be less than 1%, as previously argued.

A fine-splitting of less than 1% is observed among $v_2\{4\}$, $v_2\{6\}$ and $v_2\{8\}$, as it can be seen from their ratios, shown in figure 11 for both collision energies. The ratios $v_2\{6\}/v_2\{4\}$ and $v_2\{8\}/v_2\{4\}$ at $\sqrt{s_{NN}} = 5.02\,\mathrm{TeV}$ show a significant centrality dependence: the deviations of the ratios from unity is about 0.2% in central and increases up to about 1% for mid-central collisions. A further increase seems to be observed for more peripheral collisions, up to about 2% for centralities above 50%. The systematic uncertainties on these ratios are greatly reduced with respect to those on $v_2\{m\}$ ($m = 2, 4, 6, 8$), since the dominant
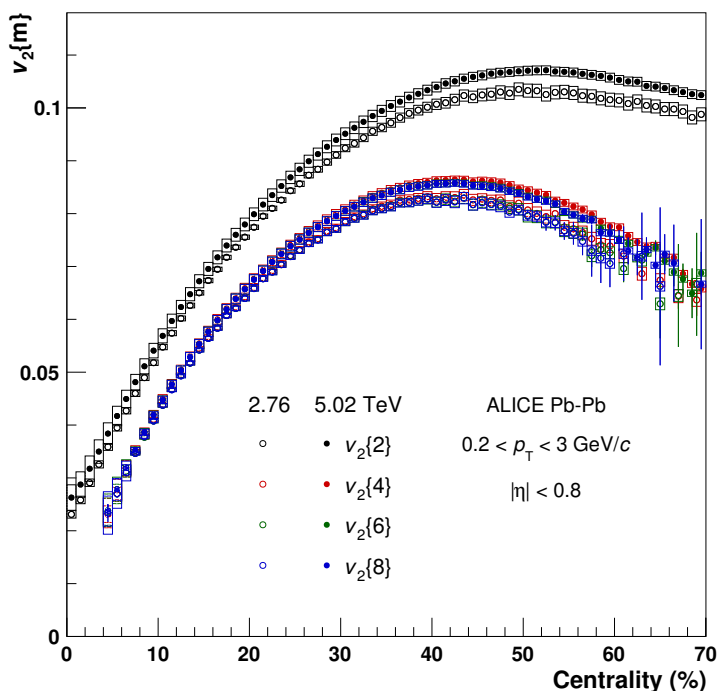
Figure 9. Elliptic flow coefficient v_2 of inclusive charged particles as a function of centrality, measured with the two- and multi-particle cumulant methods. Measurements for Pb–Pb collisions at $\sqrt{s_{NN}} = 5.02$ (2.76) TeV are shown by solid (open) markers.

sources of systematic uncertainty (track quality variables and centrality determination) among the two- and multi-particle cumulants are highly correlated. This fine-splitting is consistent with non-Bessel-Gaussian behaviour of event-by-event flow fluctuations, as previously explained. These ratios are found to be independent of the choice of p_T range within $0.2 < p_T < 3 \, \mathrm{GeV}/c$, indicating that the characterization of flow fluctuations at low p_T does not depend on p_T, even for such fine-splitting. Results at $\sqrt{s_{NN}} = 2.76 \, \mathrm{TeV}$ are found to be compatible, indicating that these ratios do not change significantly across collision energies. Compared to calculations [30] employing MC-Glauber initial conditions [80] and viscous hydrodynamics (v-USPhydro) for Pb–Pb collisions at $\sqrt{s_{NN}} = 2.76 \, \mathrm{TeV}$, the ratios $v_2\{6\}/v_2\{4\}$ and $v_2\{8\}/v_2\{4\}$ are found to be compatible. A good agreement is found between the results at $\sqrt{s_{NN}} = 2.76 \, \mathrm{TeV}$ and corresponding ATLAS results on elliptic flow p.d.f. obtained via the unfolding technique [29], as shown in figure 12.

Figure 13 shows the ratio between $v_2\{8\}$ and $v_2\{6\}$ at $\sqrt{s_{NN}} = 5.02 \, \mathrm{TeV}$. A hint of a further fine-splitting between these two, of the order of 0.05%, is observed. The results suggest little or no centrality dependence within centrality 10–50%. This difference is also consistent with non-Bessel-Gaussian elliptic flow fluctuations, and can be attributed to different contributions of the skewness to these higher-order cumulants [30]. Corresponding results at $\sqrt{s_{NN}} = 2.76 \, \mathrm{TeV}$, here and in the following, are not shown because of the large statistical uncertainties. Figure 14 shows $v_2\{6\} - v_2\{8\}$ and $(v_2\{4\} - v_2\{6\})/11$ at
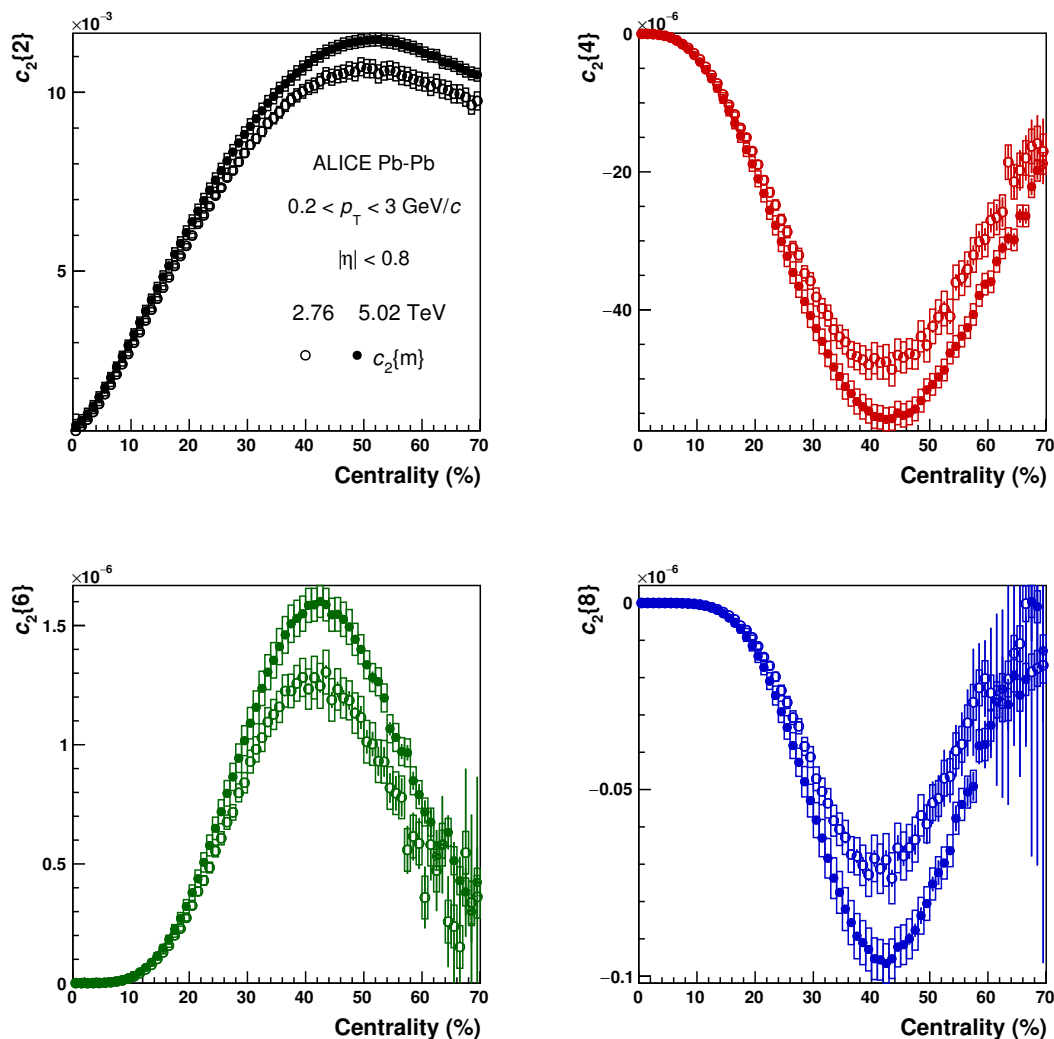
Figure 10. Cumulants c_2 of elliptic flow of inclusive charged particles as a function of centrality, for the two-particle and multi-particle cumulant methods. Measurements for Pb–Pb collisions at $\sqrt{s_{\rm NN}} = 5.02$ (2.76) TeV are shown by solid (open) markers.

$\sqrt{s_{\rm NN}} = 5.02$ TeV: these two are observed to be in agreement, which demonstrates the validity of eq. (1.8). This observation sets an upper limit of 4×10^{-4} at 95% confidence level for possible contributions to multi-particle cumulants from higher moments of the flow p.d.f. (kurtosis and beyond) in the centrality range 10–50%. This estimate is obtained assuming gaussian systematic uncertainties and summing them in quadrature with the statistical ones.

Figure 15 shows the measurement of the standardised skewness ($\gamma_1^{\rm exp}$) at $\sqrt{s_{\rm NN}} = 5.02$ TeV as a function of centrality. To suppress non-flow contributions, the values of $v_2\{2, |\Delta\eta| > 1\}$ from figure 1 are used for $v_2\{2\}$ in eq. (1.7). A negative value of the skewness, with a strong centrality dependence, is observed: $\gamma_1^{\rm exp}$ decreases from zero in central to about -0.4 in peripheral collisions. Compared to model calculations [30] for Pb–Pb collisions at $\sqrt{s_{\rm NN}} = 2.76$ TeV, the results are found to be compatible for the
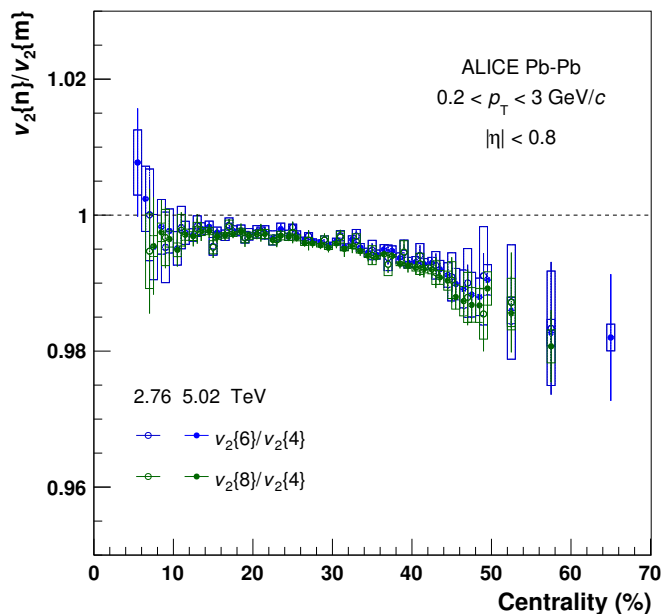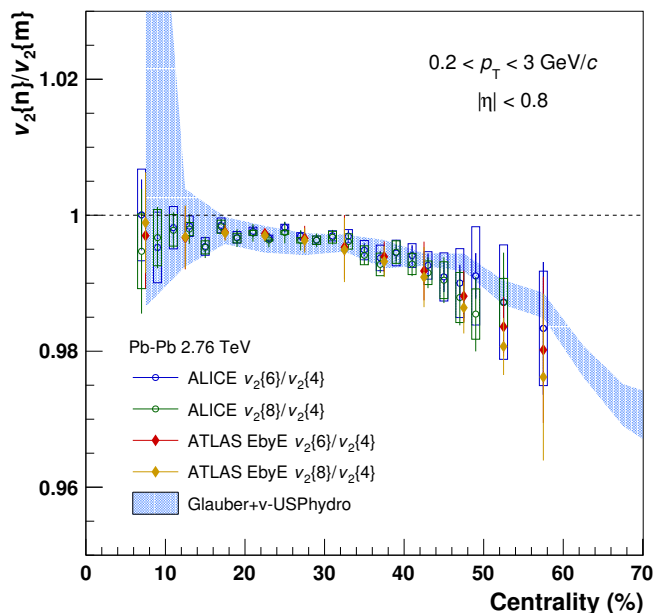
Figure 11. Ratios of elliptic flow coefficients v_2 of inclusive charged particles between measurements with different multi-particle cumulant methods, as a function of centrality. Measurements at $\sqrt{s_{\mathrm{NN}}} = 5.02$ (2.76) TeV are shown by solid (open) markers.

Figure 12. Ratios of elliptic flow coefficients v_2 of inclusive charged particles between measurements with different multi-particle cumulant methods, as a function of centrality, at $\sqrt{s_{\mathrm{NN}}} = 2.76$ TeV. Hydrodynamic calculations [30] and ATLAS measurements [29] are shown for comparison.
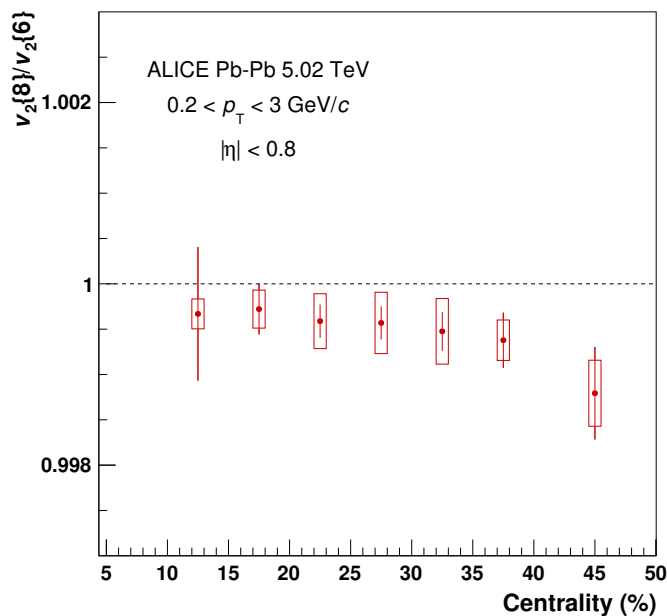
Figure 13. Ratio of elliptic flow coefficients $v_2\{8\}/v_2\{6\}$ of inclusive charged particles as a function of centrality.
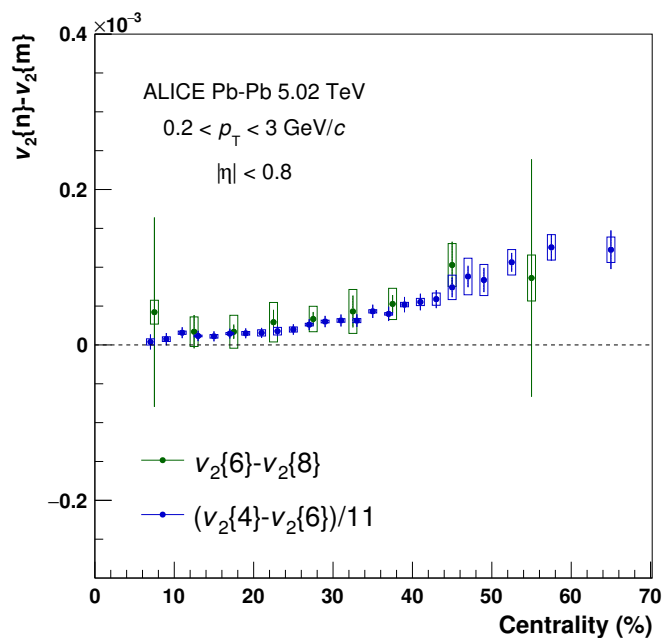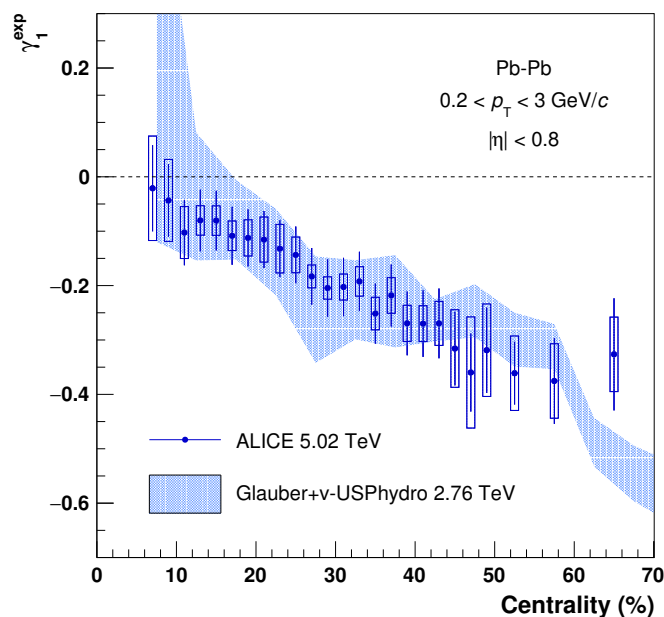

Figure 14. Differences of elliptic flow coefficients v_2 of inclusive charged particles between measurements with different multi-particle cumulant methods, as a function of centrality.

Figure 15. Skewness of elliptic flow $\gamma_1^{\rm exp}$ of inclusive charged particles as a function of centrality, for Pb–Pb collisions at $\sqrt{s_{\rm NN}} = 5.02\,{\rm TeV}$. Hydrodynamic calculations [30] for Pb–Pb collisions at $\sqrt{s_{\rm NN}} = 2.76\,{\rm TeV}$ are shown for comparison.

entire centrality range. This observation is consistent with the elliptic flow p.d.f. being progressively more left-skewed going from central to peripheral collisions. We attribute this feature to the combination of an increase in $\langle \varepsilon_2 \rangle$ and the geometrical constrain $\varepsilon_2 < 1$, as previously argued.

In order to report the full p.d.f. of elliptic flow $P(v_2)$, which can be compared to previous experimental results and theoretical predictions, it is parametrised with the Elliptic Power distribution [26, 27]

$$P(v_2) = \frac{{\rm d}\varepsilon_2}{{\rm d}v_2}\,P(\varepsilon_2) = \frac{1}{k_2}\,P\left(\frac{v_2}{k_2}\right) = \frac{2\alpha v_2}{\pi k_2^2}\,(1 - \varepsilon_0^2)^{\alpha+1/2} \int_0^\pi \frac{(1 - v_2^2/k_2^2)^{\alpha-1}}{(1 - v_2\varepsilon_0\cos\varphi/k_2)^{2\alpha+1}}\,{\rm d}\varphi, \tag{4.1}$$

and its three free parameters (α, ε_0 and k_2) are extracted from fits to the elliptic flow cumulants $c_2\{2, |\Delta\eta| > 1\}$ and $c_2\{m\}$ ($m = 4, 6, 8$) at $\sqrt{s_{\rm NN}} = 5.02\,{\rm TeV}$. The parameter α quantifies the magnitude of elliptic flow fluctuations, ε_0 the mean eccentricity in the reaction plane and k_2 is the proportionality coefficient between initial-state eccentricity and v_2 coefficient: $v_2 = k_2\varepsilon_2$. The relation between cumulants and Elliptic Power parameters is given by [27]

$$c_2\{2\} = k_2^2\,(1 - f_1), \tag{4.2}$$

$$c_2\{4\} = -k_2^4\,\left(1 - 2f_1 + 2f_1^2 - f_2\right), \tag{4.3}$$

$$c_2\{6\} = k_2^6\,\left(4 + 18f_1^2 - 12f_1^3 + 12f_1(3f_2 - 1) - 6f_2 - f_3\right), \tag{4.4}$$

$$c_2\{8\} = -k_2^8\,(33 - 288f_1^3 + 144f_1^4 - 66f_2 + 18f_2^2 - 24f_1^2(-11 + 6f_2)$$
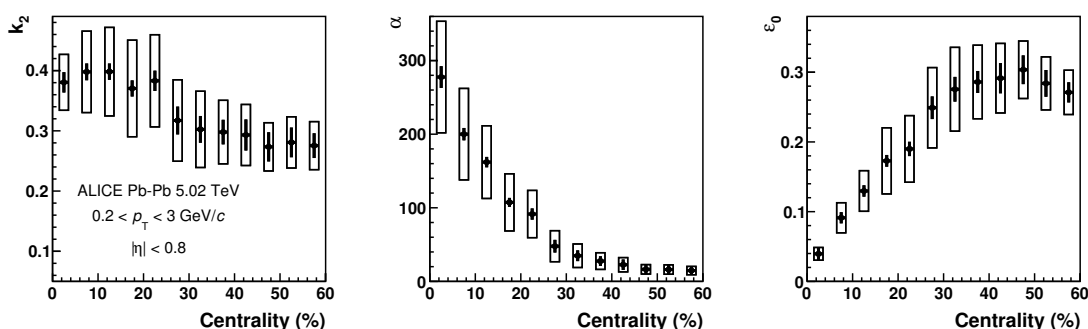$$- 12f_3 + 4f_1(-33 + 42f_2 + 4f_3) - f_4) \tag{4.5}$$

– 19 –

Figure 16. Elliptic power parameters k_2, α and ε_0 as a function of centrality, for Pb–Pb collisions at $\sqrt{s_{NN}} = 5.02\,\text{TeV}$, extracted from measurements of v_2 of inclusive charged particles with two-particle and multi-particle cumulant methods.

where

$$f_k \equiv \langle (1 - \varepsilon_n^2)^k \rangle = \frac{\alpha}{\alpha + k} \left(1 - \varepsilon_0^2\right)^k {}_2F_1\left(k + \frac{1}{2}, k; \alpha + k + 1, \varepsilon_0^2\right) \tag{4.6}$$

and ${}_2F_1$ is the hypergeometric function. The results are shown in figure 16. The systematic uncertainties are assigned varying the fit ranges and initial values of the parameters and shifting the data points according to the corresponding systematic uncertainties. An additional source of uncertainty, which is investigated, is a possible cubic response coefficient k_2', defined as $v_2 = k_2\varepsilon_2 + k_2'\varepsilon_2^3$. This coefficient is introduced to quantify the possible increase of flow fluctuations that the hydrodynamic expansion of the medium introduces with respect to geometrical fluctuations in the initial state and was argued to be non-zero in mid-central and peripheral collisions due to general properties of the hydrodynamic phase [81]. In particular, k_2' is expected to be ≤ 0.15 in the centrality range 0–60% [81]. The residual differences in α, ε_0 and k_2 when including k_2' as an additional free parameter are considered in the systematic uncertainties. The statistical uncertainties are evaluated using the subsampling method: the analysed dataset is divided into 10 sub-samples and $v_2\{m\}$ is measured in each of them. The Elliptic Power parameters are then extracted in each subsample and their dispersion is used to estimate the statistical uncertainties.

The resulting p.d.f., constructed using the Elliptic Power distribution (eq. (4.1)) with the parameters shown in figure 16 and scaled by its mean ($\langle v_2 \rangle$), is reported in figure 17, for centralities 5–10%, 25–30% and 45–50%. The systematic uncertainties take into account the correlation of the uncertainties of the Elliptic Power parameters. Other centrality ranges that are not shown here are reported in the appendix A. Scaling by $\langle v_2 \rangle$ allows a comparison of our data with results by the ATLAS collaboration [70] obtained in different p_T ranges. The observed agreement is also consistent, as previously noted, with elliptic flow fluctuations at low p_T not depending on p_T and not changing significantly between collision energies, except for the trivial increase in p_T-integrated v_2 due to the change in $\langle p_T \rangle$. Comparison with iEBE-VISHNU model calculations with AMPT and TRENTo initial conditions [62] indicates that TRENTo initial conditions are better at describing the experimental data. The data are found to be in agreement also with predictions from
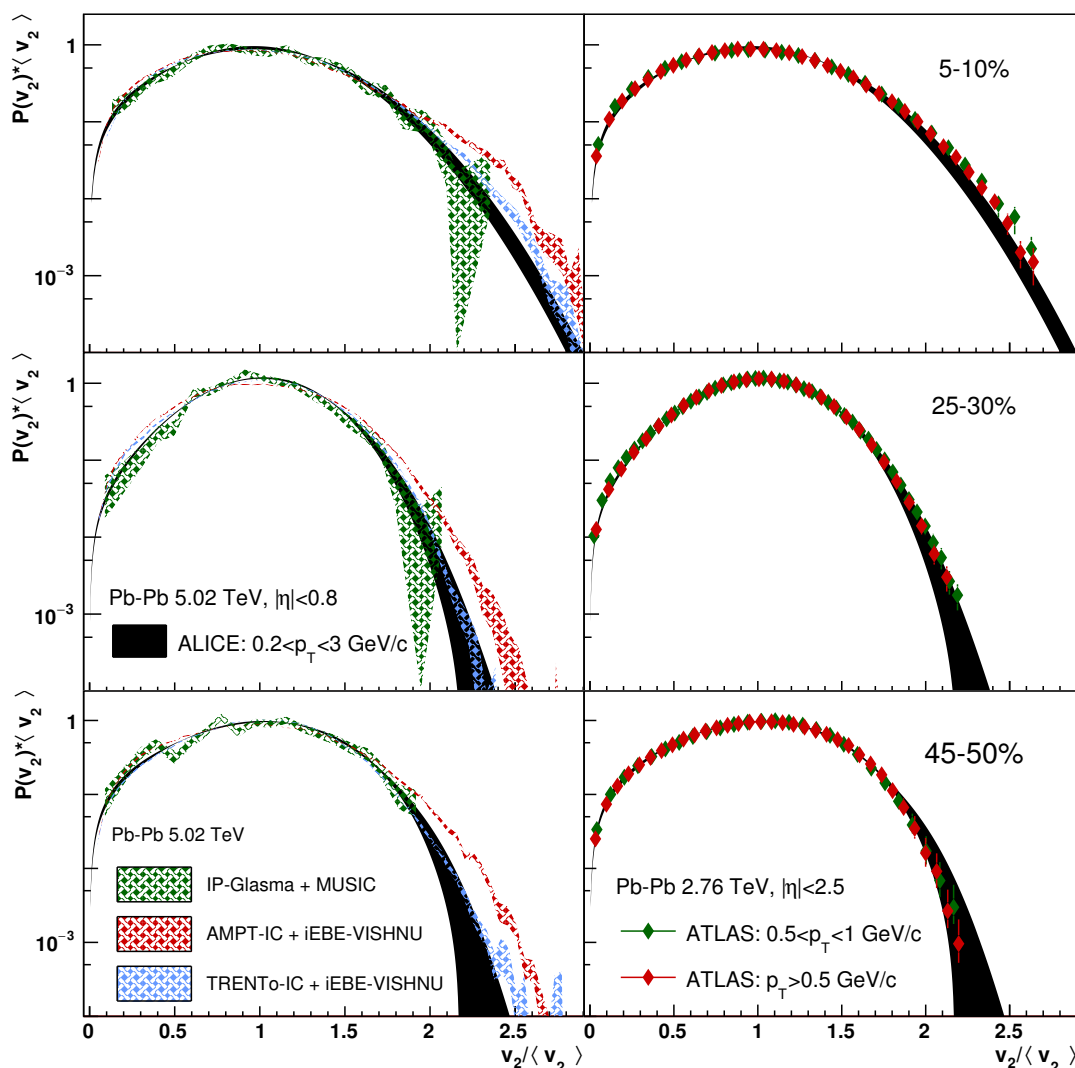
Figure 17. Elliptic flow p.d.f. $P(v_2)$ rescaled by the mean v_2 ($\langle v_2 \rangle$) of inclusive charged particles for Pb–Pb collisions at $\sqrt{s_{NN}} = 5.02$ TeV, in different centrality classes. Several hydrodynamic calculations [61, 62] and previous measurements from ATLAS [70] at lower energies are shown for comparison.

the IP-Glasma+MUSIC model [61] (with initial conditions very similar to the TRENTo ones), although the uncertainties on the theoretical predictions do not allow to draw firm conclusions.

5 Conclusions

Anisotropic flow coefficients are measured up to the sixth harmonic for inclusive charged particles at mid-rapidity ($|\eta| < 0.8$), in a wide centrality (0–80%) and p_T ($0.2 < p_T < 50$ GeV/c) ranges, for Pb–Pb collisions at $\sqrt{s_{NN}} = 5.02$ and 2.76 TeV. Comparing the results at $\sqrt{s_{NN}} = 5.02$ and 2.76 TeV the energy dependence of anisotropic flow at the LHC is

investigated. Comparison with different model calculations demonstrates that these measurements have the potential to constrain initial-state fluctuations, transport parameters of the medium and path-length dependence of energy loss of high-$p_{\rm T}$ partons. The evolution of $v_n(p_{\rm T})$ with respect to centrality and harmonic number n is also investigated. Flow coefficient of all harmonics are observed to follow an approximate power-law scaling of the form $v_n(p_{\rm T}) \sim p_{\rm T}^{n/3}$ in the $p_{\rm T}$ range $0.2 < p_{\rm T} < 3\,{\rm GeV}/c$. The ratios $v_n/v_m^{n/m}$ $n = 3, 4$ and $m = 2, 3$ are also observed to be independent of $p_{\rm T}$ within the same $p_{\rm T}$ range and show deviations of about 10% for $3 < p_{\rm T} < 10\,{\rm GeV}/c$.

The fluctuations of elliptic flow are investigated through the fine-splitting of the higher-order multi-particle cumulants ($v_2\{4\}$, $v_2\{6\}$, $v_2\{8\}$), from which the standardised skewness ($\gamma_1^{\rm exp}$) of the flow p.d.f. is extracted. Results are found to be compatible both with predictions from hydrodynamical models and with previous ATLAS results at lower energies. It is concluded that the characterization of elliptic flow fluctuations at low $p_{\rm T}$ does not depend on the $p_{\rm T}$ range and on the collision energy, except for the increase in $p_{\rm T}$-integrated v_2 due to the change in $\langle p_{\rm T} \rangle$. Direct constraints on the contribution of higher moments to the multi-particle cumulants are also reported. Finally, the full elliptic flow p.d.f., parametrised with the Elliptic Power distribution, is reported in the centrality ranges 0–60%. These results are also found to be in agreement with previous experimental results. Overall, calculations including initial conditions matching the IP-Glasma description are observed to better reproduce the elliptic flow p.d.f. while failing to describe the $p_{\rm T}$ dependence of anisotropic flow coefficients, whereas the opposite situation is observed for calculations that employ AMPT initial conditions.

Acknowledgments

A Additional figures

The elliptic flow p.d.f. $P(v_2)$, constructed as explained in section 4, in the centrality ranges not shown in figure 17 are reported in figure 18–20.
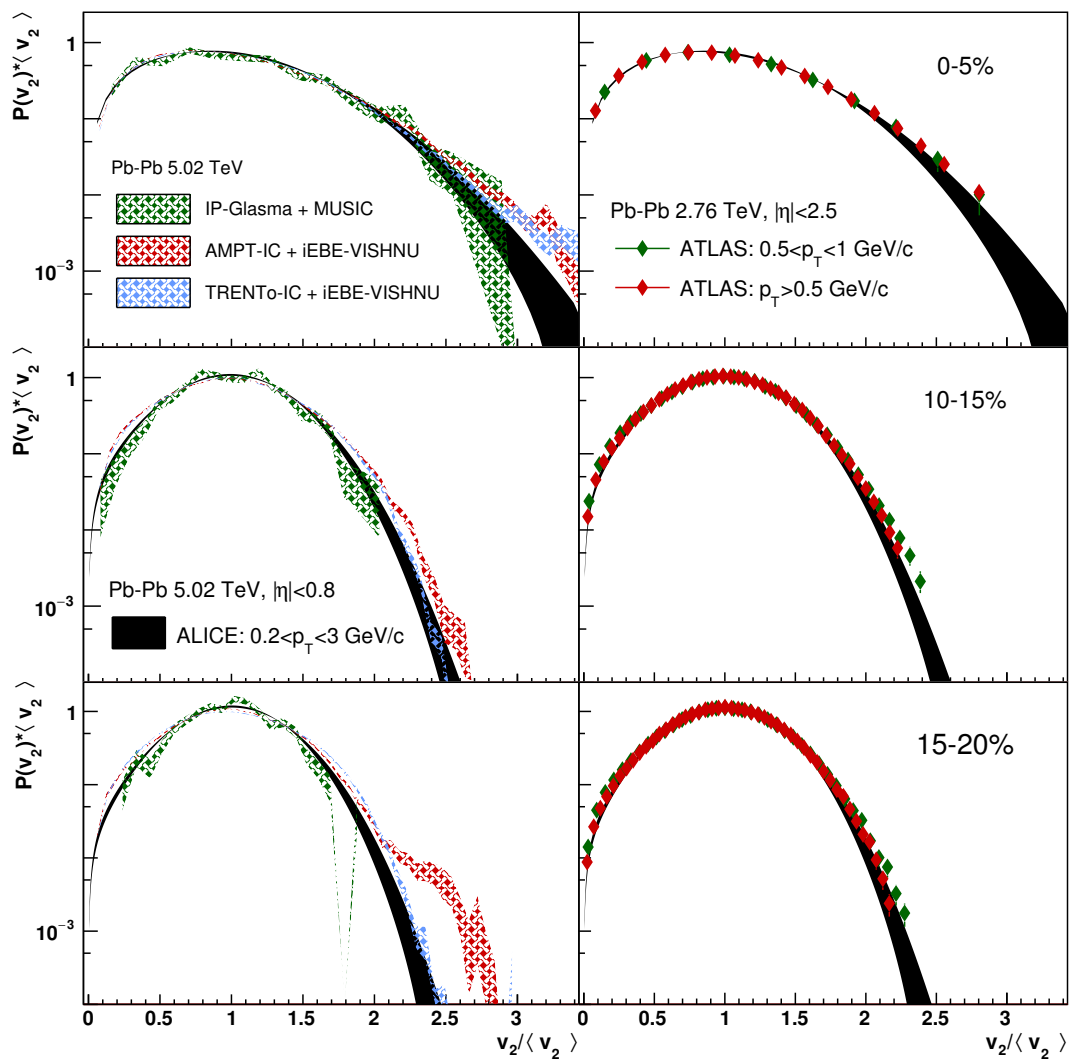
Figure 18. Elliptic flow p.d.f. $P(v_2)$ rescaled by $\langle v_2 \rangle$ in centralities 0–5%, 10–15% and 15–20% for Pb–Pb collisions at $\sqrt{s_{NN}} = 5.02\,\mathrm{TeV}$.
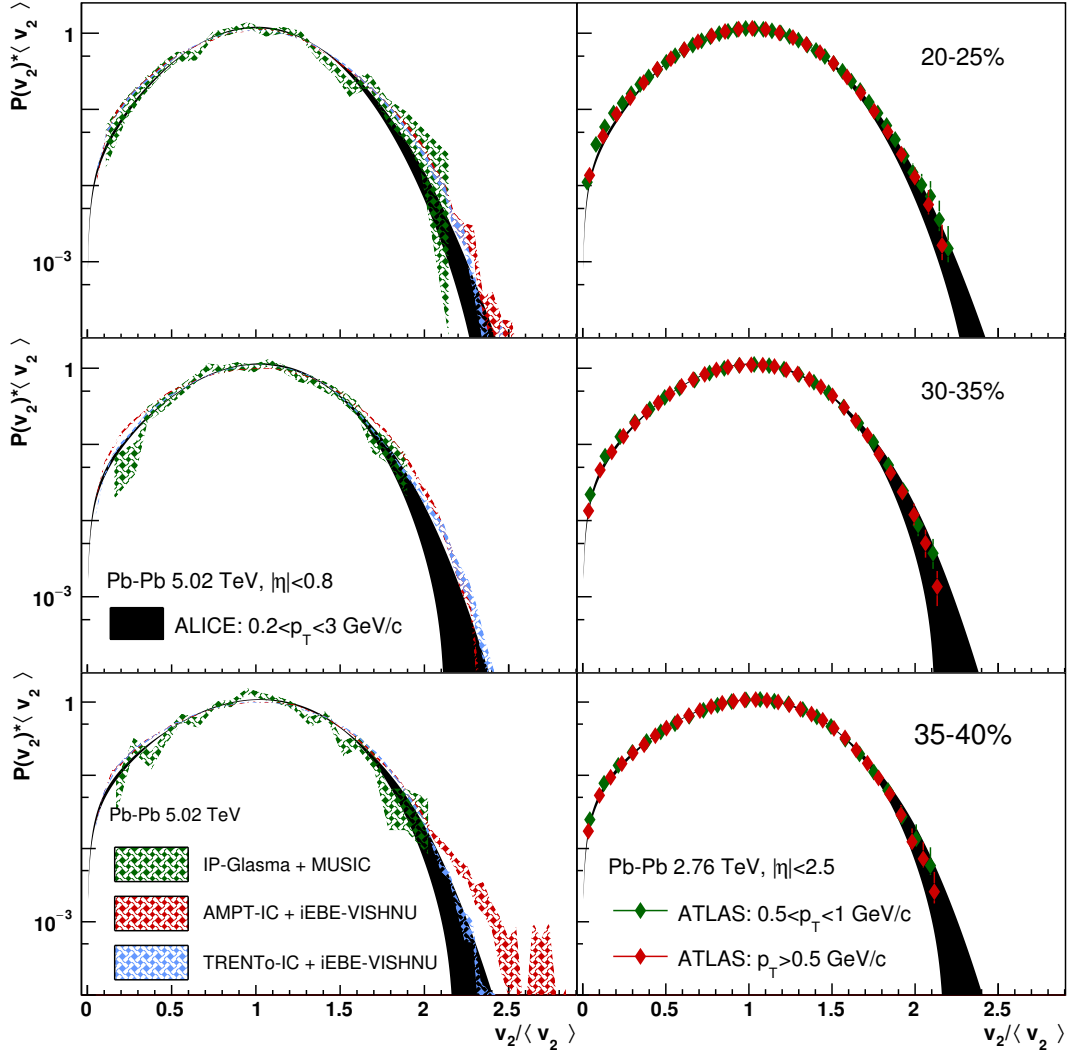
Figure 19. Elliptic flow p.d.f. $P(v_2)$ rescaled by $\langle v_2 \rangle$ in centralities 20–25%, 30–35% and 35–40% for Pb–Pb collisions at $\sqrt{s_{\mathrm{NN}}} = 5.02\,\mathrm{TeV}$.
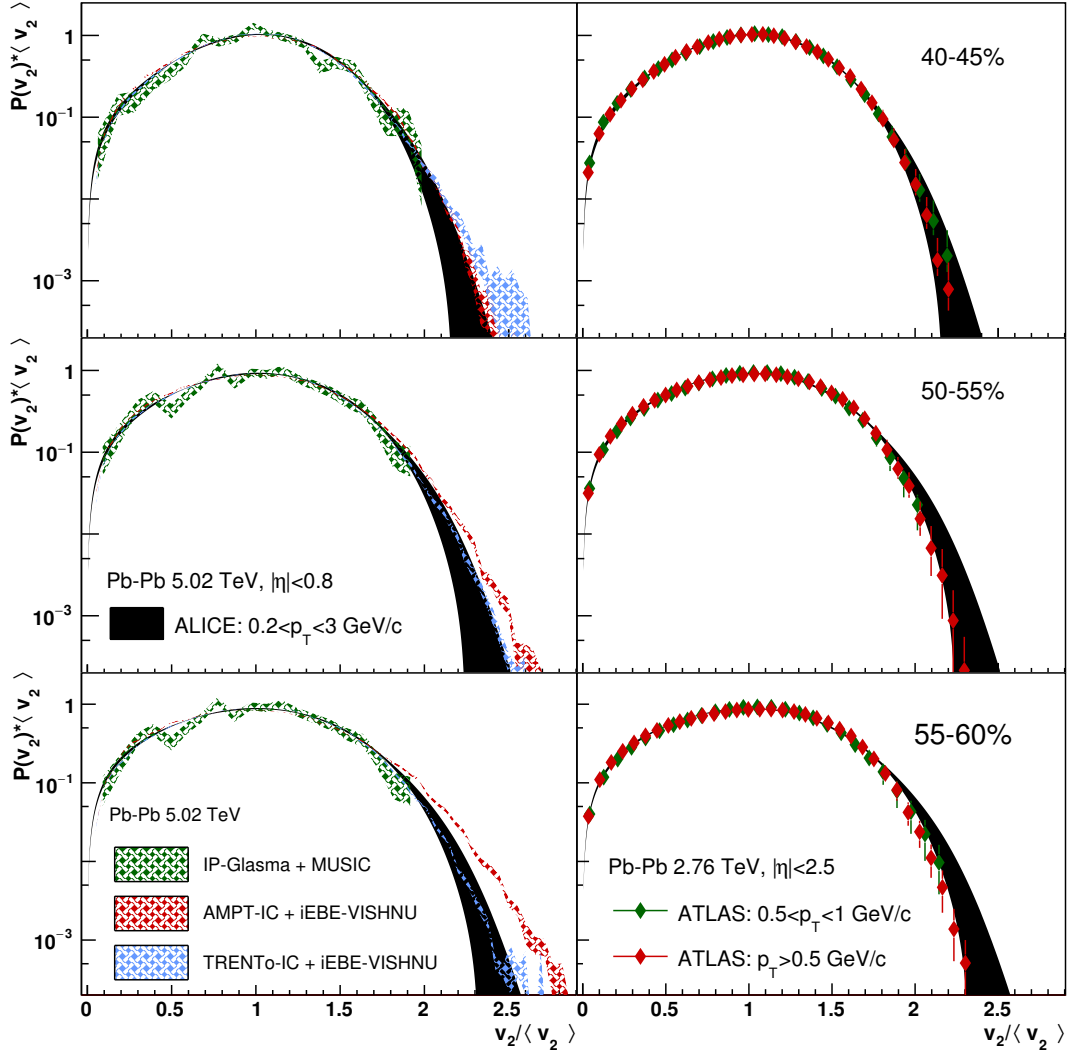
Figure 20. Elliptic flow p.d.f. $P(v_2)$ rescaled by $\langle v_2 \rangle$ in centralities 40–45%, 50–55% and 55–60% for Pb–Pb collisions at $\sqrt{s_{\mathrm{NN}}} = 5.02\,\mathrm{TeV}$.

References

[1] J.-Y. Ollitrault, *Anisotropy as a signature of transverse collective flow*, *Phys. Rev.* **D 46** (1992) 229 [inSPIRE].

[2] S.A. Voloshin, A.M. Poskanzer and and R. Snellings, *Collective phenomena in non-central nuclear collisions*, *Landolt-Bornstein* **23** (2010) 293 [arXiv:0809.2949].

[3] PHOBOS collaboration, B. Alver et al., *System size, energy, pseudorapidity and centrality dependence of elliptic flow*, *Phys. Rev. Lett.* **98** (2007) 242302 [nucl-ex/0610037] [inSPIRE].

[4] PHOBOS collaboration, B. Alver et al., *Importance of correlations and fluctuations on the initial source eccentricity in high-energy nucleus-nucleus collisions*, *Phys. Rev.* **C 77** (2008) 014906 [arXiv:0711.3724] [inSPIRE].

[5] B. Alver and G. Roland, *Collision geometry fluctuations and triangular flow in heavy-ion collisions*, *Phys. Rev.* **C 81** (2010) 054905 [*Erratum ibid.* **C 82** (2010) 039903] [arXiv:1003.0194] [inSPIRE].

[6] ALICE collaboration, *Higher harmonic anisotropic flow measurements of charged particles in Pb-Pb collisions at $\sqrt{s_{\mathrm{NN}}} = 2.76$ TeV*, *Phys. Rev. Lett.* **107** (2011) 032301 [arXiv:1105.3865] [inSPIRE].

[7] ATLAS collaboration, *Measurement of the azimuthal anisotropy for charged particle production in $\sqrt{s_{\mathrm{NN}}} = 2.76$ TeV lead-lead collisions with the ATLAS detector*, *Phys. Rev.* **C 86** (2012) 014907 [arXiv:1203.3087] [inSPIRE].

[8] CMS collaboration, *Measurement of higher-order harmonic azimuthal anisotropy in Pb-Pb collisions at $\sqrt{s_{\mathrm{NN}}} = 2.76$ TeV*, *Phys. Rev.* **C 89** (2014) 044906 [arXiv:1310.8651] [inSPIRE].

[9] M. Luzum and P. Romatschke, *Conformal relativistic viscous hydrodynamics: applications to RHIC results at $\sqrt{s_{\mathrm{NN}}} = 200$ GeV*, *Phys. Rev.* **C 78** (2008) 034915 [*Erratum ibid.* **C 79** (2009) 039903] [arXiv:0804.4015] [inSPIRE].

[10] S. Voloshin and Y. Zhang, *Flow study in relativistic nuclear collisions by Fourier expansion of Azimuthal particle distributions*, *Z. Phys.* **C 70** (1996) 665 [hep-ph/9407282] [inSPIRE].

[11] T. Hirano et al., *Hadronic dissipative effects on elliptic flow in ultrarelativistic heavy-ion collisions*, *Phys. Lett.* **B 636** (2006) 299 [nucl-th/0511046] [inSPIRE].

[12] P. Romatschke, *New developments in relativistic viscous hydrodynamics*, *Int. J. Mod. Phys.* **E 19** (2010) 1 [arXiv:0902.3663] [inSPIRE].

[13] C. Shen, U. Heinz, P. Huovinen and H. Song, *Systematic parameter study of hadron spectra and elliptic flow from viscous hydrodynamic simulations of Au+Au collisions at $\sqrt{s_{\mathrm{NN}}} = 200$ GeV*, *Phys. Rev.* **C 82** (2010) 054904 [arXiv:1010.1856] [inSPIRE].

[14] S. Ryu et al., *Importance of the bulk viscosity of QCD in ultrarelativistic heavy-ion collisions*, *Phys. Rev. Lett.* **115** (2015) 132301 [arXiv:1502.01675] [inSPIRE].

[15] S. Pratt, E. Sangaline, P. Sorensen and H. Wang, *Constraining the eq. of state of super-hadronic matter from heavy-ion collisions*, *Phys. Rev. Lett.* **114** (2015) 202301 [arXiv:1501.04042] [INSPIRE].

[16] J.E. Bernhard, J.S. Moreland, S.A. Bass, J. Liu and U. Heinz, *Applying Bayesian parameter estimation to relativistic heavy-ion collisions: simultaneous characterization of the initial state and quark-gluon plasma medium*, *Phys. Rev.* **C 94** (2016) 024907 [arXiv:1605.03954] [INSPIRE].

[17] J. Auvinen, J.E. Bernhard, S.A. Bass and I. Karpenko, *Investigating the collision energy dependence of η/s in the beam energy scan at the BNL Relativistic Heavy Ion Collider using Bayesian statistics*, *Phys. Rev.* **C 97** (2018) 044905 [arXiv:1706.03666] [INSPIRE].

[18] H. Niemi, K.J. Eskola, R. Paatelainen and K. Tuominen, *Predictions for 5.023 TeV Pb+Pb collisions at the CERN Large Hadron Collider*, *Phys. Rev.* **C 93** (2016) 014912 [arXiv:1511.04296] [INSPIRE].

[19] J. Noronha-Hostler, M. Luzum and J.-Y. Ollitrault, *Hydrodynamic predictions for 5.02 TeV Pb-Pb collisions*, *Phys. Rev.* **C 93** (2016) 034912 [arXiv:1511.06289] [INSPIRE].

[20] F.G. Gardim, F. Grassi, M. Luzum and J.-Y. Ollitrault, *Mapping the hydrodynamic response to the initial geometry in heavy-ion collisions*, *Phys. Rev.* **C 85** (2012) 024908 [arXiv:1111.6538] [INSPIRE].

[21] STAR collaboration, G. Agakishiev et al., *Energy and system-size dependence of two- and four-particle v_2 measurements in heavy-ion collisions at RHIC and their implications on flow fluctuations and nonflow*, *Phys. Rev.* **C 86** (2012) 014904 [arXiv:1111.5637] [INSPIRE].

[22] PHOBOS collaboration, B. Alver et al., *Non-flow correlations and elliptic flow fluctuations in gold-gold collisions at $\sqrt{s_{NN}} = 200$ GeV*, *Phys. Rev.* **C 81** (2010) 034915 [arXiv:1002.0534] [INSPIRE].

[23] PHOBOS collaboration, B. Alver et al., *Event-by-event fluctuations of azimuthal particle anisotropy in Au+Au collisions at $\sqrt{s_{NN}} = 200$ GeV*, *Phys. Rev. Lett.* **104** (2010) 142301 [nucl-ex/0702036] [INSPIRE].

[24] ALICE collaboration, *Elliptic flow of charged particles in Pb-Pb collisions at 2.76 TeV*, *Phys. Rev. Lett.* **105** (2010) 252302 [arXiv:1011.3914] [INSPIRE].

[25] S.A. Voloshin, A.M. Poskanzer, A. Tang and G. Wang, *Elliptic flow in the Gaussian model of eccentricity fluctuations*, *Phys. Lett.* **B 659** (2008) 537 [arXiv:0708.0800] [INSPIRE].

[26] L. Yan and J.-Y. Ollitrault, *Universal fluctuation-driven eccentricities in proton-proton, proton-nucleus and nucleus-nucleus collisions*, *Phys. Rev. Lett.* **112** (2014) 082301 [arXiv:1312.6555] [INSPIRE].

[27] L. Yan, J.-Y. Ollitrault and A.M. Poskanzer, *Eccentricity distributions in nucleus-nucleus collisions*, *Phys. Rev.* **C 90** (2014) 024903 [arXiv:1405.6595] [INSPIRE].

[28] H. Grönqvist, J.-P. Blaizot and J.-Y. Ollitrault, *Non-gaussian eccentricity fluctuations*, *Phys. Rev.* **C 94** (2016) 034905 [arXiv:1604.07230] [INSPIRE].

[29] ATLAS collaboration, *Measurement of flow harmonics with multi-particle cumulants in Pb+Pb collisions at $\sqrt{s_{NN}} = 2.76$ TeV with the ATLAS detector*, *Eur. Phys. J.* **C 74** (2014) 3157 [arXiv:1408.4342] [INSPIRE].

[30] G. Giacalone, L. Yan, J. Noronha-Hostler and J.-Y. Ollitrault, *Skewness of elliptic flow fluctuations*, *Phys. Rev.* **C 95** (2017) 014913 [arXiv:1608.01823] [INSPIRE].

[31] ALICE collaboration, *Multiparticle azimuthal correlations in p-Pb and Pb-Pb collisions at the CERN Large Hadron Collider*, *Phys. Rev.* **C 90** (2014) 054901 [arXiv:1406.2474] [inSPIRE].

[32] L. Yan, J.-Y. Ollitrault and A.M. Poskanzer, *Azimuthal anisotropy distributions in high-energy collisions*, *Phys. Lett.* **B 742** (2015) 290 [arXiv:1408.0921] [inSPIRE].

[33] J. Jia and S. Radhakrishnan, *Limitation of multiparticle correlations for studying the event-by-event distribution of harmonic flow in heavy-ion collisions*, *Phys. Rev.* **C 92** (2015) 024911 [arXiv:1412.4759] [inSPIRE].

[34] M. Gyulassy, I. Vitev and X.N. Wang, *High p_T azimuthal asymmetry in noncentral A+A at RHIC*, *Phys. Rev. Lett.* **86** (2001) 2537 [nucl-th/0012092] [inSPIRE].

[35] X.-N. Wang, *Jet quenching and azimuthal anisotropy of large p_T spectra in noncentral high-energy heavy ion collisions*, *Phys. Rev.* **C 63** (2001) 054902 [nucl-th/0009019] [inSPIRE].

[36] E.V. Shuryak, *The azimuthal asymmetry at large p_T seem to be too large for a 'jet quenching'*, *Phys. Rev.* **C 66** (2002) 027902 [nucl-th/0112042] [inSPIRE].

[37] ATLAS collaboration, *Measurement of the azimuthal angle dependence of inclusive jet yields in Pb+Pb collisions at $\sqrt{s_{NN}} = 2.76$ TeV with the ATLAS detector*, *Phys. Rev. Lett.* **111** (2013) 152301 [arXiv:1306.6469] [inSPIRE].

[38] ALICE collaboration, *Azimuthal anisotropy of charged jet production in $\sqrt{s_{NN}} = 2.76$ TeV Pb-Pb collisions*, *Phys. Lett.* **B 753** (2016) 511 [arXiv:1509.07334] [inSPIRE].

[39] CMS collaboration, *Azimuthal anisotropy of charged particles with transverse momentum up to 100 GeV/c in PbPb collisions at $\sqrt{s_{NN}} = 5.02$ TeV*, *Phys. Lett.* **B 776** (2018) 195 [arXiv:1702.00630] [inSPIRE].

[40] CMS collaboration, *Non-Gaussian elliptic-flow fluctuations in PbPb collisions at $\sqrt{s_{NN}} = 5.02$ TeV*, arXiv:1711.05594 [inSPIRE].

[41] ALICE collaboration, *Performance of the ALICE experiment at the CERN LHC*, *Int. J. Mod. Phys.* **A 29** (2014) 1430044 [arXiv:1402.4476] [inSPIRE].

[42] ALICE collaboration, *The ALICE experiment at the CERN LHC*, 2008 *JINST* **3** S08002 [inSPIRE].

[43] ALICE collaboration, *Centrality determination of Pb-Pb collisions at $\sqrt{s_{NN}} = 2.76$ TeV with ALICE*, *Phys. Rev.* **C 88** (2013) 044909 [arXiv:1301.4361] [inSPIRE].

[44] A. Bilandzic, R. Snellings and S. Voloshin, *Flow analysis with cumulants: direct calculations*, *Phys. Rev.* **C 83** (2011) 044913 [arXiv:1010.0233] [inSPIRE].

[45] A. Bilandzic et al., *Generic framework for anisotropic flow analyses with multiparticle azimuthal correlations*, *Phys. Rev.* **C 89** (2014) 064904 [arXiv:1312.3572] [inSPIRE].

[46] STAR collaboration, C. Adler et al., *Elliptic flow from two and four particle correlations in Au+Au collisions at $\sqrt{s_{NN}} = 130$ GeV*, *Phys. Rev.* **C 66** (2002) 034904 [nucl-ex/0206001] [inSPIRE].

[47] M. Luzum and J.-Y. Ollitrault, *Eliminating experimental bias in anisotropic-flow measurements of high-energy nuclear collisions*, *Phys. Rev.* **C 87** (2013) 044907 [arXiv:1209.2323] [inSPIRE].

[48] R. Barlow, *Systematic errors: Facts and fictions*, in the proceedings of the *Conference on Statistical Techniques in Particle Physics*, March 18–22, Durhamm, U.K. (2002), hep-ex/0207026 [INSPIRE].

[49] ALICE collaboration, *Anisotropic flow of charged particles in Pb-Pb collisions at $\sqrt{s_{NN}} = 5.02$ TeV*, *Phys. Rev. Lett.* **116** (2016) 132302 [arXiv:1602.01119] [INSPIRE].

[50] STAR collaboration, K.H. Ackermann et al., *Elliptic flow in Au + Au collisions at $\sqrt{s_{NN}} = 130$ GeV*, *Phys. Rev. Lett.* **86** (2001) 402 [nucl-ex/0009011] [INSPIRE].

[51] K.J. Eskola, K. Kajantie, P.V. Ruuskanen and K. Tuominen, *Scaling of transverse energies and multiplicities with atomic number and energy in ultrarelativistic nuclear collisions*, *Nucl. Phys.* **B 570** (2000) 379 [hep-ph/9909456] [INSPIRE].

[52] H. Niemi, K.J. Eskola and R. Paatelainen, *Event-by-event fluctuations in a perturbative QCD + saturation + hydrodynamics model: Determining QCD matter shear viscosity in ultrarelativistic heavy-ion collisions*, *Phys. Rev.* **C 93** (2016) 024907 [arXiv:1505.02677] [INSPIRE].

[53] N. Borghini and J.-Y. Ollitrault, *Momentum spectra, anisotropic flow and ideal fluids*, *Phys. Lett.* **B 642** (2006) 227 [nucl-th/0506045] [INSPIRE].

[54] B.H. Alver, C. Gombeaud, M. Luzum and J.-Y. Ollitrault, *Triangular flow in hydrodynamics and transport theory*, *Phys. Rev.* **C 82** (2010) 034913 [arXiv:1007.5469] [INSPIRE].

[55] D. Teaney, *The effects of viscosity on spectra, elliptic flow and HBT radii*, *Phys. Rev.* **C 68** (2003) 034913 [nucl-th/0301099] [INSPIRE].

[56] Z. Qiu and U.W. Heinz, *Event-by-event shape and flow fluctuations of relativistic heavy-ion collision fireballs*, *Phys. Rev.* **C 84** (2011) 024911 [arXiv:1104.0650] [INSPIRE].

[57] C. Andrés, M. Braun and C. Pajares, *Energy loss as the origin of a universal scaling law of the elliptic flow*, *Eur. Phys. J.* **A 53** (2017) 41 [arXiv:1609.03927] [INSPIRE].

[58] F.G. Gardim, F. Grassi, M. Luzum and J.-Y. Ollitrault, *Breaking of factorization of two-particle correlations in hydrodynamics*, *Phys. Rev.* **C 87** (2013) 031901 [arXiv:1211.0989] [INSPIRE].

[59] CMS collaboration, *Evidence for transverse momentum and pseudorapidity dependent event plane fluctuations in PbPb and pPb collisions*, *Phys. Rev.* **C 92** (2015) 034911 [arXiv:1503.01692] [INSPIRE].

[60] J. Bartels, K.J. Golec-Biernat and H. Kowalski, *A modification of the saturation model: DGLAP evolution*, *Phys. Rev.* **D 66** (2002) 014001 [hep-ph/0203258] [INSPIRE].

[61] S. McDonald et al., *Phys. Rev.* **C 95** (2017) 064913 [arXiv:1609.02958] [INSPIRE].

[62] W. Zhao, H.-j. Xu and H. Song, *Collective flow in 2.76 A TeV and 5.02 A TeV Pb+Pb collisions*, *Eur. Phys. J.* **C 77** (2017) 645 [arXiv:1703.10792] [INSPIRE].

[63] Z.-W. Lin et al., *A Multi-phase transport model for relativistic heavy ion collisions*, *Phys. Rev.* **C 72** (2005) 064901 [nucl-th/0411110] [INSPIRE].

[64] J.S. Moreland, J.E. Bernhard and S.A. Bass, *Alternative ansatz to wounded nucleon and binary collision scaling in high-energy nuclear collisions*, *Phys. Rev.* **C 92** (2015) 011901 [arXiv:1412.4708] [INSPIRE].

[65] S.A. Bass et al., *Microscopic models for ultrarelativistic heavy ion collisions*, *Prog. Part. Nucl. Phys.* **41** (1998) 255 [nucl-th/9803035] [INSPIRE].

[66] B. Betz et al., *Cumulants and nonlinear response of high p_T harmonic flow at $\sqrt{s_{NN}} = 5.02$ TeV*, *Phys. Rev.* **C 95** (2017) 044901 [arXiv:1609.05171] [INSPIRE].

[67] J. Noronha-Hostler et al., *Bulk viscosity effects in event-by-event relativistic hydrodynamics*, *Phys. Rev.* **C 88** (2013) 044916 [arXiv:1305.1981] [INSPIRE].

[68] B. Betz, M. Gyulassy and G. Torrieri, *Fourier harmonics of high-p_T particles probing the fluctuating intitial condition geometries in heavy-ion collisions*, *Phys. Rev.* **C 84** (2011) 024913 [arXiv:1102.5416] [INSPIRE].

[69] R.J. Fries, V. Greco, and P. Sorensen, *Coalescence models for hadron formation from quark gluon plasma*, *Ann. Rev. Nucl. Part. Sci.* **58** (2008) 177 [arXiv:0807.4939].

[70] ATLAS collaboration, *Measurement of the distributions of event-by-event flow harmonics in lead-lead collisions at = 2.76 TeV with the ATLAS detector at the LHC*, *JHEP* **11** (2013) 183 [arXiv:1305.2942] [INSPIRE].

[71] ALICE collaboration, *Event shape engineering for inclusive spectra and elliptic flow in Pb-Pb collisions at $\sqrt{s_{NN}} = 2.76$ TeV*, *Phys. Rev.* **C 93** (2016) 034916 [arXiv:1507.06194] [INSPIRE].

[72] J. Schukraft, A. Timmins and S.A. Voloshin, *Ultra-relativistic nuclear collisions: event shape engineering*, *Phys. Lett.* **B 719** (2013) 394 [arXiv:1208.4563] [INSPIRE].

[73] ALICE collaboration, *Anisotropic flow of charged hadrons, pions and (anti-)protons measured at high transverse momentum in Pb-Pb collisions at $\sqrt{s_{NN}} = 2.76$ TeV*, *Phys. Lett.* **B 719** (2013) 18 [arXiv:1205.5761] [INSPIRE].

[74] STAR collaboration, J. Adams et al., *Azimuthal anisotropy at RHIC: the first and fourth harmonics*, *Phys. Rev. Lett.* **92** (2004) 062301 [nucl-ex/0310029] [INSPIRE].

[75] PHENIX collaboration, A. Adare et al., *Elliptic and hexadecapole flow of charged hadrons in Au+Au collisions at $\sqrt{s_{NN}} = 200$ GeV*, *Phys. Rev. Lett.* **105** (2010) 062301 [arXiv:1003.5586] [INSPIRE].

[76] C. Gombeaud and J.-Y. Ollitrault, *Effects of flow fluctuations and partial thermalization on v(4)*, *Phys. Rev.* **C 81** (2010) 014901 [arXiv:0907.4664] [INSPIRE].

[77] P.F. Kolb, L.-W. Chen, V. Greco and C.M. Ko, *Momentum anisotropies in the quark coalescence model*, *Phys. Rev.* **C 69** (2004) 051901 [nucl-th/0402049] [INSPIRE].

[78] P. Liu and R.A. Lacey, *Acoustic scaling of linear and mode-coupled anisotropic flow; implications for precision extraction of the specific shear viscosity*, arXiv:1802.06595 [INSPIRE].

[79] R.A. Lacey, A. Taranenko, N.N. Ajitanand and J.M. Alexander, *Scaling of the higher-order flow harmonics: implications for initial-eccentricity models and the 'viscous horizon'*, arXiv:1105.3782 [INSPIRE].

[80] B. Alver, M. Baker, C. Loizides and P. Steinberg, *The PHOBOS glauber Monte Carlo*, arXiv:0805.4411 [INSPIRE].

[81] J. Noronha-Hostler, L. Yan, F.G. Gardim and J.-Y. Ollitrault, *Linear and cubic response to the initial eccentricity in heavy-ion collisions*, *Phys. Rev.* **C 93** (2016) 014909 [arXiv:1511.03896] [INSPIRE].

The ALICE collaboration

S. Acharya[138] , F.T.-. Acosta[22] , D. Adamová[93] , J. Adolfsson[80] , M.M. Aggarwal[97] , G. Aglieri Rinella[36] , M. Agnello[33] , N. Agrawal[48] , Z. Ahammed[138] , S.U. Ahn[76] , S. Aiola[143] , A. Akindinov[64] , M. Al-Turany[103] , S.N. Alam[138] , D.S.D. Albuquerque[119] , D. Aleksandrov[87] , B. Alessandro[58] , R. Alfaro Molina[72] , Y. Ali[16] , A. Alici[11 ,53 ,29] , A. Alkin[3] , J. Alme[24] , T. Alt[69] , L. Altenkamper[24] , I. Altsybeev[137] , C. Andrei[47] , D. Andreou[36] , H.A. Andrews[107] , A. Andronic[103] , M. Angeletti[36] , V. Anguelov[101] , C. Anson[17] , T. Antičić[104] , F. Antinori[56] , P. Antonioli[53] , R. Anwar[123] , N. Apadula[79] , L. Aphecetche[111] , H. Appelshäuser[69] , S. Arcelli[29] , R. Arnaldi[58] , O.W. Arnold[102 ,114] , I.C. Arsene[23] , M. Arslandok[101] , B. Audurier[111] , A. Augustinus[36] , R. Averbeck[103] , M.D. Azmi[18] , A. Badalà[55] , Y.W. Baek[60 ,41] , S. Bagnasco[58] , R. Bailhache[69] , R. Bala[98] , A. Baldisseri[134] , M. Ball[43] , R.C. Baral[85] , A.M. Barbano[28] , R. Barbera[30] , F. Barile[52] , L. Barioglio[28] , G.G. Barnaföldi[142] , L.S. Barnby[92] , V. Barret[131] , P. Bartalini[7] , K. Barth[36] , E. Bartsch[69] , N. Bastid[131] , S. Basu[140] , G. Batigne[111] , B. Batyunya[75] , P.C. Batzing[23] , J.L. Bazo Alba[108] , I.G. Bearden[88] , H. Beck[101] , C. Bedda[63] , N.K. Behera[60] , I. Belikov[133] , F. Bellini[29 ,36] , H. Bello Martinez[2] , R. Bellwied[123] , L.G.E. Beltran[117] , V. Belyaev[91] , G. Bencedi[142] , S. Beole[28] , A. Bercuci[47] , Y. Berdnikov[95] , D. Berenyi[142] , R.A. Bertens[127] , D. Berzano[36 ,58] , L. Betev[36] , P.P. Bhaduri[138] , A. Bhasin[98] , I.R. Bhat[98] , H. Bhatt[48] , B. Bhattacharjee[42] , J. Bhom[115] , A. Bianchi[28] , L. Bianchi[123] , N. Bianchi[51] , J. Bielčík[38] , J. Bielčíková[93] , A. Bilandzic[102 ,114] , G. Biro[142] , R. Biswas[4] , S. Biswas[4] , J.T. Blair[116] , D. Blau[87] , C. Blume[69] , G. Boca[135] , F. Bock[36] , A. Bogdanov[91] , L. Boldizsár[142] , M. Bombara[39] , G. Bonomi[136] , M. Bonora[36] , H. Borel[134] , A. Borissov[141 ,20] , M. Borri[125] , E. Botta[28] , C. Bourjau[88] , L. Bratrud[69] , P. Braun-Munzinger[103] , M. Bregant[118] , T.A. Broker[69] , M. Broz[38] , E.J. Brucken[44] , E. Bruna[58] , G.E. Bruno[36 ,35] , D. Budnikov[105] , H. Buesching[69] , S. Bufalino[33] , P. Buhler[110] , P. Buncic[36] , O. Busch[130] , Z. Buthelezi[73] , J.B. Butt[16] , J.T. Buxton[19] , J. Cabala[113] , D. Caffarri[89] , H. Caines[143] , A. Caliva[103] , E. Calvo Villar[108] , R.S. Camacho[2] , P. Camerini[27] , A.A. Capon[110] , F. Carena[36] , W. Carena[36] , F. Carnesecchi[29 ,11] , J. Castillo Castellanos[134] , A.J. Castro[127] , E.A.R. Casula[54] , C. Ceballos Sanchez[9] , S. Chandra[138] , B. Chang[124] , W. Chang[7] , S. Chapeland[36] , M. Chartier[125] , S. Chattopadhyay[138] , S. Chattopadhyay[106] , A. Chauvin[114 ,102] , C. Cheshkov[132] , B. Cheynis[132] , V. Chibante Barroso[36] , D.D. Chinellato[119] , S. Cho[60] , P. Chochula[36] , T. Chowdhury[131] , P. Christakoglou[89] , C.H. Christensen[88] , P. Christiansen[80] , T. Chujo[130] , S.U. Chung[20] , C. Cicalo[54] , L. Cifarelli[11 ,29] , F. Cindolo[53] , J. Cleymans[122] , F. Colamaria[52] , D. Colella[65 ,52 ,36] , A. Collu[79] , M. Colocci[29] , M. Concas[58 , i] , G. Conesa Balbastre[78] , Z. Conesa del Valle[61] , J.G. Contreras[38] , T.M. Cormier[94] , Y. Corrales Morales[58] , P. Cortese[34] , M.R. Cosentino[120] , F. Costa[36] , S. Costanza[135] , J. Crkovská[61] , P. Crochet[131] , E. Cuautle[70] , L. Cunqueiro[94 ,141] , T. Dahms[102 ,114] , A. Dainese[56] , M.C. Danisch[101] , A. Danu[68] , D. Das[106] , I. Das[106] , S. Das[4] , A. Dash[85] , S. Dash[48] , S. De[49] , A. De Caro[32] , G. de Cataldo[52] , C. de Conti[118] , J. de Cuveland[40] , A. De Falco[26] , D. De Gruttola[11 ,32] , N. De Marco[58] , S. De Pasquale[32] , R.D. De Souza[119] , H.F. Degenhardt[118] , A. Deisting[103 ,101] , A. Deloff[84] , S. Delsanto[28] , C. Deplano[89] , P. Dhankher[48] , D. Di Bari[35] , A. Di Mauro[36] , B. Di Ruzza[56] , R.A. Diaz[9] , T. Dietel[122] , P. Dillenseger[69] , Y. Ding[7] , R. Divià[36] , Ø. Djuvsland[24] , A. Dobrin[36] , D. Domenicis Gimenez[118] , B. Dönigus[69] , O. Dordic[23] , L.V.R. Doremalen[63] , A.K. Dubey[138] , A. Dubla[103] , L. Ducroux[132] , S. Dudi[97] , A.K. Duggal[97] , M. Dukhishyam[85] , P. Dupieux[131] , R.J. Ehlers[143] , D. Elia[52] , E. Endress[108] , H. Engel[74] , E. Epple[143] , B. Erazmus[111] , F. Erhardt[96] , M.R. Ersdal[24] , B. Espagnon[61] , G. Eulisse[36] , J. Eum[20] , D. Evans[107] , S. Evdokimov[90] , L. Fabbietti[102 ,114] , M. Faggin[31] , J. Faivre[78] , A. Fantoni[51] , M. Fasel[94] , L. Feldkamp[141] , A. Feliciello[58] , G. Feofilov[137] , A. Fernández Téllez[2] , A. Ferretti[28] ,

A. Festanti[31],[36] , V.J.G. Feuillard[134],[131] , J. Figiel[115] , M.A.S. Figueredo[118] , S. Filchagin[105] ,
D. Finogeev[62] , F.M. Fionda[24] , G. Fiorenza[52] , M. Floris[36] , S. Foertsch[73] , P. Foka[103] ,
S. Fokin[87] , E. Fragiacomo[59] , A. Francescon[36] , A. Francisco[111] , U. Frankenfeld[103] ,
G.G. Fronze[28] , U. Fuchs[36] , C. Furget[78] , A. Furs[62] , M. Fusco Girard[32] , J.J. Gaardhøje[88] ,
M. Gagliardi[28] , A.M. Gago[108] , K. Gajdosova[88] , M. Gallio[28] , C.D. Galvan[117] , P. Ganoti[83] ,
C. Garabatos[103] , E. Garcia-Solis[12] , K. Garg[30] , C. Gargiulo[36] , P. Gasik[102],[114] , E.F. Gauger[116] ,
M.B. Gay Ducati[71] , M. Germain[111] , J. Ghosh[106] , P. Ghosh[138] , S.K. Ghosh[4] , P. Gianotti[51] ,
P. Giubellino[58],[103] , P. Giubilato[31] , P. Glässel[101] , D.M. Gómez Coral[72] , A. Gomez Ramirez[74] ,
V. Gonzalez[103] , P. González-Zamora[2] , S. Gorbunov[40] , L. Görlich[115] , S. Gotovac[126] ,
V. Grabski[72] , L.K. Graczykowski[139] , K.L. Graham[107] , L. Greiner[79] , A. Grelli[63] , C. Grigoras[36] ,
V. Grigoriev[91] , A. Grigoryan[1] , S. Grigoryan[75] , J.M. Gronefeld[103] , F. Grosa[33] ,
J.F. Grosse-Oetringhaus[36] , R. Grosso[103] , R. Guernane[78] , B. Guerzoni[29] , M. Guittiere[111] ,
K. Gulbrandsen[88] , T. Gunji[129] , A. Gupta[98] , R. Gupta[98] , I.B. Guzman[2] , R. Haake[36] ,
M.K. Habib[103] , C. Hadjidakis[61] , H. Hamagaki[81] , G. Hamar[142] , J.C. Hamon[133] , M.R. Haque[63] ,
J.W. Harris[143] , A. Harton[12] , H. Hassan[78] , D. Hatzifotiadou[53],[11] , S. Hayashi[129] , S.T. Heckel[69] ,
E. Hellbär[69] , H. Helstrup[37] , A. Herghelegiu[47] , E.G. Hernandez[2] , G. Herrera Corral[10] ,
F. Herrmann[141] , K.F. Hetland[37] , T.E. Hilden[44] , H. Hillemanns[36] , C. Hills[125] , B. Hippolyte[133] ,
B. Hohlweger[102] , D. Horak[38] , S. Hornung[103] , R. Hosokawa[130],[78] , P. Hristov[36] , C. Hughes[127] ,
P. Huhn[69] , T.J. Humanic[19] , H. Hushnud[106] , N. Hussain[42] , T. Hussain[18] , D. Hutter[40] ,
D.S. Hwang[21] , J.P. Iddon[125] , S.A. Iga Buitron[70] , R. Ilkaev[105] , M. Inaba[130] , M. Ippolitov[87] ,
M.S. Islam[106] , M. Ivanov[103] , V. Ivanov[95] , V. Izucheev[90] , B. Jacak[79] , N. Jacazio[29] ,
P.M. Jacobs[79] , M.B. Jadhav[48] , S. Jadlovska[113] , J. Jadlovsky[113] , S. Jaelani[63] ,
C. Jahnke[118],[114] , M.J. Jakubowska[139] , M.A. Janik[139] , C. Jena[85] , M. Jercic[96] , R.T. Jimenez
Bustamante[103] , M. Jin[123] , P.G. Jones[107] , A. Jusko[107] , P. Kalinak[65] , A. Kalweit[36] ,
J.H. Kang[144] , V. Kaplin[91] , S. Kar[7] , A. Karasu Uysal[77] , O. Karavichev[62] , T. Karavicheva[62] ,
P. Karczmarczyk[36] , E. Karpechev[62] , U. Kebschull[74] , R. Keidel[46] , D.L.D. Keijdener[63] ,
M. Keil[36] , B. Ketzer[43] , Z. Khabanova[89] , S. Khan[18] , S.A. Khan[138] , A. Khanzadeev[95] ,
Y. Kharlov[90] , A. Khatun[18] , A. Khuntia[49] , M.M. Kielbowicz[115] , B. Kileng[37] , B. Kim[130] ,
D. Kim[144] , D.J. Kim[124] , E.J. Kim[14] , H. Kim[144] , J.S. Kim[41] , J. Kim[101] , M. Kim[60],[101] ,
S. Kim[21] , T. Kim[144] , T. Kim[144] , S. Kirsch[40] , I. Kisel[40] , S. Kiselev[64] , A. Kisiel[139] , J.L. Klay[6] ,
C. Klein[69] , J. Klein[36],[58] , C. Klein-Bösing[141] , S. Klewin[101] , A. Kluge[36] , M.L. Knichel[36],[101] ,
A.G. Knospe[123] , C. Kobdaj[112] , M. Kofarago[142] , M.K. Köhler[101] , T. Kollegger[103] ,
N. Kondratyeva[91] , E. Kondratyuk[90] , A. Konevskikh[62] , M. Konyushikhin[140] , O. Kovalenko[84] ,
V. Kovalenko[137] , M. Kowalski[115] , I. Králik[65] , A. Kravčáková[39] , L. Kreis[103] , M. Krivda[107],[65] ,
F. Krizek[93] , M. Krüger[69] , E. Kryshen[95] , M. Krzewicki[40] , A.M. Kubera[19] , V. Kučera[60],[93] ,
C. Kuhn[133] , P.G. Kuijer[89] , J. Kumar[48] , L. Kumar[97] , S. Kumar[48] , S. Kundu[85] ,
P. Kurashvili[84] , A. Kurepin[62] , A.B. Kurepin[62] , A. Kuryakin[105] , S. Kushpil[93] , M.J. Kweon[60] ,
Y. Kwon[144] , S.L. La Pointe[40] , P. La Rocca[30] , Y.S. Lai[79] , I. Lakomov[36] , R. Langoy[121] ,
K. Lapidus[143] , C. Lara[74] , A. Lardeux[23] , P. Larionov[51] , A. Lattuca[28] , E. Laudi[36] ,
R. Lavicka[38] , R. Lea[27] , L. Leardini[101] , S. Lee[144] , F. Lehas[89] , S. Lehner[110] , J. Lehrbach[40] ,
R.C. Lemmon[92] , E. Leogrande[63] , I. León Monzón[117] , P. Lévai[142] , X. Li[13] , X.L. Li[7] ,
J. Lien[121] , R. Lietava[107] , B. Lim[20] , S. Lindal[23] , V. Lindenstruth[40] , S.W. Lindsay[125] ,
C. Lippmann[103] , M.A. Lisa[19] , V. Litichevskyi[44] , A. Liu[79] , H.M. Ljunggren[80] , W.J. Llope[140] ,
D.F. Lodato[63] , V. Loginov[91] , C. Loizides[79],[94] , P. Loncar[126] , X. Lopez[131] , E. López Torres[9] ,
A. Lowe[142] , P. Luettig[69] , J.R. Luhder[141] , M. Lunardon[31] , G. Luparello[59] , M. Lupi[36] ,
A. Maevskaya[62] , M. Mager[36] , S.M. Mahmood[23] , A. Maire[133] , R.D. Majka[143] , M. Malaev[95] ,
L. Malinina[75],[ii] , D. Mal'Kevich[64] , P. Malzacher[103] , A. Mamonov[105] , V. Manko[87] ,
F. Manso[131] , V. Manzari[52] , Y. Mao[7] , M. Marchisone[132],[128],[73] , J. Mareš[67] ,

G.V. Margagliotti[27] , A. Margotti[53] , J. Margutti[63] , A. Marín[103] , C. Markert[116] ,
M. Marquard[69] , N.A. Martin[103] , P. Martinengo[36] , M.I. Martínez[2] , G. Martínez García[111] ,
M. Martinez Pedreira[36] , S. Masciocchi[103] , M. Masera[28] , A. Masoni[54] , L. Massacrier[61] ,
E. Masson[111] , A. Mastroserio[52] , A.M. Mathis[102] [,114] , P.F.T. Matuoka[118] , A. Matyja[115] [,127] ,
C. Mayer[115] , M. Mazzilli[35] , M.A. Mazzoni[57] , F. Meddi[25] , Y. Melikyan[91] ,
A. Menchaca-Rocha[72] , E. Meninno[32] , J. Mercado Pérez[101] , M. Meres[15] , C.S. Meza[108] ,
S. Mhlanga[122] , Y. Miake[130] , L. Micheletti[28] , M.M. Mieskolainen[44] , D.L. Mihaylov[102] ,
K. Mikhaylov[64] [,75] , A. Mischke[63] , A.N. Mishra[70] , D. Miśkowiec[103] , J. Mitra[138] , C.M. Mitu[68] ,
N. Mohammadi[36] [,63] , A.P. Mohanty[63] , B. Mohanty[85] , M. Mohisin Khan[18] [, iii] , D.A. Moreira De
Godoy[141] , L.A.P. Moreno[2] , S. Moretto[31] , A. Morreale[111] , A. Morsch[36] , V. Muccifora[51] ,
E. Mudnic[126] , D. Mühlheim[141] , S. Muhuri[138] , M. Mukherjee[4] , J.D. Mulligan[143] ,
M.G. Munhoz[118] , K. Münning[43] , M.I.A. Munoz[79] , R.H. Munzer[69] , H. Murakami[129] ,
S. Murray[73] , L. Musa[36] , J. Musinsky[65] , C.J. Myers[123] , J.W. Myrcha[139] , B. Naik[48] , R. Nair[84] ,
B.K. Nandi[48] , R. Nania[53] [,11] , E. Nappi[52] , A. Narayan[48] , M.U. Naru[16] , H. Natal da Luz[118] ,
C. Nattrass[127] , S.R. Navarro[2] , K. Nayak[85] , R. Nayak[48] , T.K. Nayak[138] , S. Nazarenko[105] ,
R.A. Negrao De Oliveira[69] [,36] , L. Nellen[70] , S.V. Nesbo[37] , G. Neskovic[40] , F. Ng[123] ,
M. Nicassio[103] , J. Niedziela[139] [,36] , B.S. Nielsen[88] , S. Nikolaev[87] , S. Nikulin[87] , V. Nikulin[95] ,
F. Noferini[11] [,53] , P. Nomokonov[75] , G. Nooren[63] , J.C.C. Noris[2] , J. Norman[78] [,125] , A. Nyanin[87] ,
J. Nystrand[24] , H. Oh[144] , A. Ohlson[101] , J. Oleniacz[139] , A.C. Oliveira Da Silva[118] ,
M.H. Oliver[143] , J. Onderwaater[103] , C. Oppedisano[58] , R. Orava[44] , M. Oravec[113] , A. Ortiz
Velasquez[70] , A. Oskarsson[80] , J. Otwinowski[115] , K. Oyama[81] , Y. Pachmayer[101] , V. Pacik[88] ,
D. Pagano[136] , G. Paić[70] , P. Palni[7] , J. Pan[140] , A.K. Pandey[48] , S. Panebianco[134] ,
V. Papikyan[1] , P. Pareek[49] , J. Park[60] , J.E. Parkkila[124] , S. Parmar[97] , A. Passfeld[141] ,
S.P. Pathak[123] , R.N. Patra[138] , B. Paul[58] , H. Pei[7] , T. Peitzmann[63] , X. Peng[7] , L.G. Pereira[71] ,
H. Pereira Da Costa[134] , D. Peresunko[87] , E. Perez Lezama[69] , V. Peskov[69] , Y. Pestov[5] ,
V. Petráček[38] , M. Petrovici[47] , C. Petta[30] , R.P. Pezzi[71] , S. Piano[59] , M. Pikna[15] , P. Pillot[111] ,
L.O.D.L. Pimentel[88] , O. Pinazza[53] [,36] , L. Pinsky[123] , S. Pisano[51] , D.B. Piyarathna[123] ,
M. Płoskoń[79] , M. Planinic[96] , F. Pliquett[69] , J. Pluta[139] , S. Pochybova[142] ,
P.L.M. Podesta-Lerma[117] , M.G. Poghosyan[94] , B. Polichtchouk[90] , N. Poljak[96] ,
W. Poonsawat[112] , A. Pop[47] , H. Poppenborg[141] , S. Porteboeuf-Houssais[131] , V. Pozdniakov[75] ,
S.K. Prasad[4] , R. Preghenella[53] , F. Prino[58] , C.A. Pruneau[140] , I. Pshenichnov[62] , M. Puccio[28] ,
V. Punin[105] , J. Putschke[140] , S. Raha[4] , S. Rajput[98] , J. Rak[124] , A. Rakotozafindrabe[134] ,
L. Ramello[34] , F. Rami[133] , R. Raniwala[99] , S. Raniwala[99] , S.S. Räsänen[44] , B.T. Rascanu[69] ,
V. Ratza[43] , I. Ravasenga[33] , K.F. Read[127] [,94] , K. Redlich[84] [, iv] , A. Rehman[24] , P. Reichelt[69] ,
F. Reidt[36] , X. Ren[7] , R. Renfordt[69] , A. Reshetin[62] , J.-P. Revol[11] , K. Reygers[101] , V. Riabov[95] ,
T. Richert[63] [,80] , M. Richter[23] , P. Riedler[36] , W. Riegler[36] , F. Riggi[30] , C. Ristea[68] ,
M. Rodríguez Cahuantzi[2] , K. Røed[23] , R. Rogalev[90] , E. Rogochaya[75] , D. Rohr[36] , D. Röhrich[24] ,
P.S. Rokita[139] , F. Ronchetti[51] , E.D. Rosas[70] , K. Roslon[139] , P. Rosnet[131] , A. Rossi[56] [,31] ,
A. Rotondi[135] , F. Roukoutakis[83] , C. Roy[133] , P. Roy[106] , O.V. Rueda[70] , R. Rui[27] ,
B. Rumyantsev[75] , A. Rustamov[86] , E. Ryabinkin[87] , Y. Ryabov[95] , A. Rybicki[115] , S. Saarinen[44] ,
S. Sadhu[138] , S. Sadovsky[90] , K. Šafařík[36] , S.K. Saha[138] , B. Sahoo[48] , P. Sahoo[49] , R. Sahoo[49] ,
S. Sahoo[66] , P.K. Sahu[66] , J. Saini[138] , S. Sakai[130] , M.A. Saleh[140] , S. Sambyal[98] ,
V. Samsonov[95] [,91] , A. Sandoval[72] , A. Sarkar[73] , D. Sarkar[138] , N. Sarkar[138] , P. Sarma[42] ,
M.H.P. Sas[63] , E. Scapparone[53] , F. Scarlassara[31] , B. Schaefer[94] , H.S. Scheid[69] , C. Schiaua[47] ,
R. Schicker[101] , C. Schmidt[103] , H.R. Schmidt[100] , M.O. Schmidt[101] , M. Schmidt[100] ,
N.V. Schmidt[94] [,69] , J. Schukraft[36] , Y. Schutz[36] [,133] , K. Schwarz[103] , K. Schweda[103] ,
G. Scioli[29] , E. Scomparin[58] , M. Šefčík[39] , J.E. Seger[17] , Y. Sekiguchi[129] , D. Sekihata[45] ,
I. Selyuzhenkov[91] [,103] , K. Senosi[73] , S. Senyukov[133] , E. Serradilla[72] , P. Sett[48] , A. Sevcenco[68] ,

A. Shabanov[62], A. Shabetai[111], R. Shahoyan[36], W. Shaikh[106], A. Shangaraev[90], A. Sharma[97], A. Sharma[98], N. Sharma[97], A.I. Sheikh[138], K. Shigaki[45], M. Shimomura[82], S. Shirinkin[64], Q. Shou[7 ,109], K. Shtejer[28], Y. Sibiriak[87], S. Siddhanta[54], K.M. Sielewicz[36], T. Siemiarczuk[84], D. Silvermyr[80], G. Simatovic[89], G. Simonetti[102 ,36], R. Singaraju[138], R. Singh[85], V. Singhal[138], T. Sinha[106], B. Sitar[15], M. Sitta[34], T.B. Skaali[23], M. Slupecki[124], N. Smirnov[143], R.J.M. Snellings[63], T.W. Snellman[124], J. Song[20], F. Soramel[31], S. Sorensen[127], F. Sozzi[103], I. Sputowska[115], J. Stachel[101], I. Stan[68], P. Stankus[94], E. Stenlund[80], D. Stocco[111], M.M. Storetvedt[37], P. Strmen[15], A.A.P. Suaide[118], T. Sugitate[45], C. Suire[61], M. Suleymanov[16], M. Suljic[36 ,27], R. Sultanov[64], M. Šumbera[93], S. Sumowidagdo[50], K. Suzuki[110], S. Swain[66], A. Szabo[15], I. Szarka[15], U. Tabassam[16], J. Takahashi[119], G.J. Tambave[24], N. Tanaka[130], M. Tarhini[61 ,111], M. Tariq[18], M.G. Tarzila[47], A. Tauro[36], G. Tejeda Muñoz[2], A. Telesca[36], C. Terrevoli[31], B. Teyssier[132], D. Thakur[49], S. Thakur[138], D. Thomas[116], F. Thoresen[88], R. Tieulent[132], A. Tikhonov[62], A.R. Timmins[123], A. Toia[69], N. Topilskaya[62], M. Toppi[51], S.R. Torres[117], S. Tripathy[49], S. Trogolo[28], G. Trombetta[35], L. Tropp[39], V. Trubnikov[3], W.H. Trzaska[124], T.P. Trzcinski[139], B.A. Trzeciak[63], T. Tsuji[129], A. Tumkin[105], R. Turrisi[56], T.S. Tveter[23], K. Ullaland[24], E.N. Umaka[123], A. Uras[132], G.L. Usai[26], A. Utrobicic[96], M. Vala[113], J.W. Van Hoorne[36], M. van Leeuwen[63], P. Vande Vyvre[36], D. Varga[142], A. Vargas[2], M. Vargyas[124], R. Varma[48], M. Vasileiou[83], A. Vasiliev[87], A. Vauthier[78], O. Vázquez Doce[102 ,114], V. Vechernin[137], A.M. Veen[63], A. Velure[24], E. Vercellin[28], S. Vergara Limón[2], L. Vermunt[63], R. Vernet[8], R. Vértesi[142], L. Vickovic[126], J. Viinikainen[124], Z. Vilakazi[128], O. Villalobos Baillie[107], A. Villatoro Tello[2], A. Vinogradov[87], T. Virgili[32], V. Vislavicius[80], A. Vodopyanov[75], M.A. Völkl[100], K. Voloshin[64], S.A. Voloshin[140], G. Volpe[35], B. von Haller[36], I. Vorobyev[114 ,102], D. Voscek[113], D. Vranic[103 ,36], J. Vrláková[39], B. Wagner[24], H. Wang[63], M. Wang[7], Y. Watanabe[130 ,129], M. Weber[110], S.G. Weber[103], A. Wegrzynek[36], D.F. Weiser[101], S.C. Wenzel[36], J.P. Wessels[141], U. Westerhoff[141], A.M. Whitehead[122], J. Wiechula[69], J. Wikne[23], G. Wilk[84], J. Wilkinson[53], G.A. Willems[141 ,36], M.C.S. Williams[53], E. Willsher[107], B. Windelband[101], W.E. Witt[127], R. Xu[7], S. Yalcin[77], K. Yamakawa[45], S. Yano[45], Z. Yin[7], H. Yokoyama[130 ,78], I.-K. Yoo[20], J.H. Yoon[60], V. Yurchenko[3], V. Zaccolo[58], A. Zaman[16], C. Zampolli[36], H.J.C. Zanoli[118], N. Zardoshti[107], A. Zarochentsev[137], P. Závada[67], N. Zaviyalov[105], H. Zbroszczyk[139], M. Zhalov[95], X. Zhang[7], Y. Zhang[7], Z. Zhang[131 ,7], C. Zhao[23], V. Zherebchevskii[137], N. Zhigareva[64], D. Zhou[7], Y. Zhou[88], Z. Zhou[24], H. Zhu[7], J. Zhu[7], Y. Zhu[7], A. Zichichi[29 ,11], M.B. Zimmermann[36], G. Zinovjev[3], J. Zmeskal[110], S. Zou[7],

[i] *Dipartimento DET del Politecnico di Torino, Turin, Italy*
[ii] *M.V. Lomonosov Moscow State University, D.V. Skobeltsyn Institute of Nuclear, Physics, Moscow, Russia*
[iii] *Department of Applied Physics, Aligarh Muslim University, Aligarh, India*
[iv] *Institute of Theoretical Physics, University of Wroclaw, Poland*

[1] *A.I. Alikhanyan National Science Laboratory (Yerevan Physics Institute) Foundation, Yerevan, Armenia*
[2] *Benemérita Universidad Autónoma de Puebla, Puebla, Mexico*
[3] *Bogolyubov Institute for Theoretical Physics, National Academy of Sciences of Ukraine, Kiev, Ukraine*
[4] *Bose Institute, Department of Physics and Centre for Astroparticle Physics and Space Science (CAPSS), Kolkata, India*
[5] *Budker Institute for Nuclear Physics, Novosibirsk, Russia*

6   *California Polytechnic State University, San Luis Obispo, California, United States*
7   *Central China Normal University, Wuhan, China*
8   *Centre de Calcul de l'IN2P3, Villeurbanne, Lyon, France*
9   *Centro de Aplicaciones Tecnológicas y Desarrollo Nuclear (CEADEN), Havana, Cuba*
10 *Centro de Investigación y de Estudios Avanzados (CINVESTAV), Mexico City and Mérida, Mexico*
11 *Centro Fermi - Museo Storico della Fisica e Centro Studi e Ricerche "Enrico Fermi", Rome, Italy*
12 *Chicago State University, Chicago, Illinois, United States*
13 *China Institute of Atomic Energy, Beijing, China*
14 *Chonbuk National University, Jeonju, Republic of Korea*
15 *Comenius University Bratislava, Faculty of Mathematics, Physics and Informatics, Bratislava, Slovakia*
16 *COMSATS Institute of Information Technology (CIIT), Islamabad, Pakistan*
17 *Creighton University, Omaha, Nebraska, United States*
18 *Department of Physics, Aligarh Muslim University, Aligarh, India*
19 *Department of Physics, Ohio State University, Columbus, Ohio, United States*
20 *Department of Physics, Pusan National University, Pusan, Republic of Korea*
21 *Department of Physics, Sejong University, Seoul, Republic of Korea*
22 *Department of Physics, University of California, Berkeley, California, United States*
23 *Department of Physics, University of Oslo, Oslo, Norway*
24 *Department of Physics and Technology, University of Bergen, Bergen, Norway*
25 *Dipartimento di Fisica dell'Università 'La Sapienza' and Sezione INFN, Rome, Italy*
26 *Dipartimento di Fisica dell'Università and Sezione INFN, Cagliari, Italy*
27 *Dipartimento di Fisica dell'Università and Sezione INFN, Trieste, Italy*
28 *Dipartimento di Fisica dell'Università and Sezione INFN, Turin, Italy*
29 *Dipartimento di Fisica e Astronomia dell'Università and Sezione INFN, Bologna, Italy*
30 *Dipartimento di Fisica e Astronomia dell'Università and Sezione INFN, Catania, Italy*
31 *Dipartimento di Fisica e Astronomia dell'Università and Sezione INFN, Padova, Italy*
32 *Dipartimento di Fisica 'E.R. Caianiello' dell'Università and Gruppo Collegato INFN, Salerno, Italy*
33 *Dipartimento DISAT del Politecnico and Sezione INFN, Turin, Italy*
34 *Dipartimento di Scienze e Innovazione Tecnologica dell'Università del Piemonte Orientale and INFN Sezione di Torino, Alessandria, Italy*
35 *Dipartimento Interateneo di Fisica 'M. Merlin' and Sezione INFN, Bari, Italy*
36 *European Organization for Nuclear Research (CERN), Geneva, Switzerland*
37 *Faculty of Engineering and Science, Western Norway University of Applied Sciences, Bergen, Norway*
38 *Faculty of Nuclear Sciences and Physical Engineering, Czech Technical University in Prague, Prague, Czech Republic*
39 *Faculty of Science, P.J. Šafárik University, Košice, Slovakia*
40 *Frankfurt Institute for Advanced Studies, Johann Wolfgang Goethe-Universität Frankfurt, Frankfurt, Germany*
41 *Gangneung-Wonju National University, Gangneung, Republic of Korea*
42 *Gauhati University, Department of Physics, Guwahati, India*
43 *Helmholtz-Institut für Strahlen- und Kernphysik, Rheinische Friedrich-Wilhelms-Universität Bonn, Bonn, Germany*
44 *Helsinki Institute of Physics (HIP), Helsinki, Finland*
45 *Hiroshima University, Hiroshima, Japan*
46 *Hochschule Worms, Zentrum für Technologietransfer und Telekommunikation (ZTT), Worms, Germany*
47 *Horia Hulubei National Institute of Physics and Nuclear Engineering, Bucharest, Romania*
48 *Indian Institute of Technology Bombay (IIT), Mumbai, India*
49 *Indian Institute of Technology Indore, Indore, India*
50 *Indonesian Institute of Sciences, Jakarta, Indonesia*

[51] INFN, Laboratori Nazionali di Frascati, Frascati, Italy
[52] INFN, Sezione di Bari, Bari, Italy
[53] INFN, Sezione di Bologna, Bologna, Italy
[54] INFN, Sezione di Cagliari, Cagliari, Italy
[55] INFN, Sezione di Catania, Catania, Italy
[56] INFN, Sezione di Padova, Padova, Italy
[57] INFN, Sezione di Roma, Rome, Italy
[58] INFN, Sezione di Torino, Turin, Italy
[59] INFN, Sezione di Trieste, Trieste, Italy
[60] Inha University, Incheon, Republic of Korea
[61] Institut de Physique Nucléaire d'Orsay (IPNO), Institut National de Physique Nucléaire et de Physique des Particules (IN2P3/CNRS), Université de Paris-Sud, Université Paris-Saclay, Orsay, France
[62] Institute for Nuclear Research, Academy of Sciences, Moscow, Russia
[63] Institute for Subatomic Physics, Utrecht University/Nikhef, Utrecht, Netherlands
[64] Institute for Theoretical and Experimental Physics, Moscow, Russia
[65] Institute of Experimental Physics, Slovak Academy of Sciences, Košice, Slovakia
[66] Institute of Physics, Bhubaneswar, India
[67] Institute of Physics of the Czech Academy of Sciences, Prague, Czech Republic
[68] Institute of Space Science (ISS), Bucharest, Romania
[69] Institut für Kernphysik, Johann Wolfgang Goethe-Universität Frankfurt, Frankfurt, Germany
[70] Instituto de Ciencias Nucleares, Universidad Nacional Autónoma de México, Mexico City, Mexico
[71] Instituto de Física, Universidade Federal do Rio Grande do Sul (UFRGS), Porto Alegre, Brazil
[72] Instituto de Física, Universidad Nacional Autónoma de México, Mexico City, Mexico
[73] iThemba LABS, National Research Foundation, Somerset West, South Africa
[74] Johann-Wolfgang-Goethe Universität Frankfurt Institut für Informatik, Fachbereich Informatik und Mathematik, Frankfurt, Germany
[75] Joint Institute for Nuclear Research (JINR), Dubna, Russia
[76] Korea Institute of Science and Technology Information, Daejeon, Republic of Korea
[77] KTO Karatay University, Konya, Turkey
[78] Laboratoire de Physique Subatomique et de Cosmologie, Université Grenoble-Alpes, CNRS-IN2P3, Grenoble, France
[79] Lawrence Berkeley National Laboratory, Berkeley, California, United States
[80] Lund University Department of Physics, Division of Particle Physics, Lund, Sweden
[81] Nagasaki Institute of Applied Science, Nagasaki, Japan
[82] Nara Women's University (NWU), Nara, Japan
[83] National and Kapodistrian University of Athens, School of Science, Department of Physics , Athens, Greece
[84] National Centre for Nuclear Research, Warsaw, Poland
[85] National Institute of Science Education and Research, HBNI, Jatni, India
[86] National Nuclear Research Center, Baku, Azerbaijan
[87] National Research Centre Kurchatov Institute, Moscow, Russia
[88] Niels Bohr Institute, University of Copenhagen, Copenhagen, Denmark
[89] Nikhef, National institute for subatomic physics, Amsterdam, Netherlands
[90] NRC 'Kurchatov Institute' IHEP, Protvino, Russia
[91] NRNU Moscow Engineering Physics Institute, Moscow, Russia
[92] Nuclear Physics Group, STFC Daresbury Laboratory, Daresbury, United Kingdom
[93] Nuclear Physics Institute of the Czech Academy of Sciences, Řež u Prahy, Czech Republic
[94] Oak Ridge National Laboratory, Oak Ridge, Tennessee, United States
[95] Petersburg Nuclear Physics Institute, Gatchina, Russia
[96] Physics department, Faculty of science, University of Zagreb, Zagreb, Croatia
[97] Physics Department, Panjab University, Chandigarh, India

98   *Physics Department, University of Jammu, Jammu, India*
99   *Physics Department, University of Rajasthan, Jaipur, India*
100   *Physikalisches Institut, Eberhard-Karls-Universität Tübingen, Tübingen, Germany*
101   *Physikalisches Institut, Ruprecht-Karls-Universität Heidelberg, Heidelberg, Germany*
102   *Physik Department, Technische Universität München, Munich, Germany*
103   *Research Division and ExtreMe Matter Institute EMMI, GSI Helmholtzzentrum für Schwerionenforschung GmbH, Darmstadt, Germany*
104   *Rudjer Bošković Institute, Zagreb, Croatia*
105   *Russian Federal Nuclear Center (VNIIEF), Sarov, Russia*
106   *Saha Institute of Nuclear Physics, Kolkata, India*
107   *School of Physics and Astronomy, University of Birmingham, Birmingham, United Kingdom*
108   *Sección Física, Departamento de Ciencias, Pontificia Universidad Católica del Perú, Lima, Peru*
109   *Shanghai Institute of Applied Physics, Shanghai, China*
110   *Stefan Meyer Institut für Subatomare Physik (SMI), Vienna, Austria*
111   *SUBATECH, IMT Atlantique, Université de Nantes, CNRS-IN2P3, Nantes, France*
112   *Suranaree University of Technology, Nakhon Ratchasima, Thailand*
113   *Technical University of Košice, Košice, Slovakia*
114   *Technische Universität München, Excellence Cluster 'Universe', Munich, Germany*
115   *The Henryk Niewodniczanski Institute of Nuclear Physics, Polish Academy of Sciences, Cracow, Poland*
116   *The University of Texas at Austin, Austin, Texas, United States*
117   *Universidad Autónoma de Sinaloa, Culiacán, Mexico*
118   *Universidade de São Paulo (USP), São Paulo, Brazil*
119   *Universidade Estadual de Campinas (UNICAMP), Campinas, Brazil*
120   *Universidade Federal do ABC, Santo Andre, Brazil*
121   *University College of Southeast Norway, Tonsberg, Norway*
122   *University of Cape Town, Cape Town, South Africa*
123   *University of Houston, Houston, Texas, United States*
124   *University of Jyväskylä, Jyväskylä, Finland*
125   *University of Liverpool, Department of Physics Oliver Lodge Laboratory , Liverpool, United Kingdom*
126   *University of Split, Faculty of Electrical Engineering, Mechanical Engineering and Naval Architecture, Split, Croatia*
127   *University of Tennessee, Knoxville, Tennessee, United States*
128   *University of the Witwatersrand, Johannesburg, South Africa*
129   *University of Tokyo, Tokyo, Japan*
130   *University of Tsukuba, Tsukuba, Japan*
131   *Université Clermont Auvergne, CNRS/IN2P3, LPC, Clermont-Ferrand, France*
132   *Université de Lyon, Université Lyon 1, CNRS/IN2P3, IPN-Lyon, Villeurbanne, Lyon, France*
133   *Université de Strasbourg, CNRS, IPHC UMR 7178, F-67000 Strasbourg, France, Strasbourg, France*
134   *Université Paris-Saclay Centre d'Études de Saclay (CEA), IRFU, Department de Physique Nucléaire (DPhN), Saclay, France*
135   *Università degli Studi di Pavia, Pavia, Italy*
136   *Università di Brescia, Brescia, Italy*
137   *V. Fock Institute for Physics, St. Petersburg State University, St. Petersburg, Russia*
138   *Variable Energy Cyclotron Centre, Kolkata, India*
139   *Warsaw University of Technology, Warsaw, Poland*
140   *Wayne State University, Detroit, Michigan, United States*
141   *Westfälische Wilhelms-Universität Münster, Institut für Kernphysik, Münster, Germany*
142   *Wigner Research Centre for Physics, Hungarian Academy of Sciences, Budapest, Hungary*
143   *Yale University, New Haven, Connecticut, United States*
144   *Yonsei University, Seoul, Republic of Korea*